Hydroecology and Engineering

SCIEPublish

Article

Comparative Runoff Hydrology Modeling and Hydropower Potential Analysis Under Climate Change: A Case Study of the Dudhkoshi River Basin

Sambridhi Karki [1,*], Aditya Dhakal [1,*], Saroj Karki [2,*] and Bishnu Prasad Shrestha [1,*]

[1] Department of Agricultural Engineering, Purwanchal Campus, Institute of Engineering, Tribhuvan University, Dharan 56700, Nepal

[2] Ministry of Water Supply, Irrigation, and Energy, Biratnagar 56613, Nepal

* Corresponding author. E-mail: sambridhi79lwe@ioepc.edu.np (S.K.); ard@ioepc.edu.np (A.D.); sarojioe@gmail.com (S.K.); bishnu79lwe@ioepc.edu.np (B.P.S.)

Received: 21 August 2026; Revised: 23 September 2026; Accepted: 30 October 2026; Available online: 12 November 2026

ABSTRACT: Nepal's abundant rivers offer immense hydropower potential, yet accurately estimating runoff and hydropower feasibility remains challenging because of complex terrain, limited data, and climate variability. This study compares the Hydrologic Engineering Center–Hydrologic Modeling System (HEC-HMS) and the Soil and Water Assessment Tool (SWAT) to simulate runoff and evaluate hydropower potential in the Dudhkoshi River Basin, eastern Nepal. The HEC-HMS model, a semi-distributed, event-based framework, was used to simulate rainfall-runoff processes, while SWAT, a continuous, physically-based model, was employed for long-term hydrological simulation, hydropower site identification, and climate change impact assessment. The basin was delineated into 395 sub-basins and 4822 Hydrologic Response Units (HRUs) using a Digital Elevation Model (DEM), land use, soil, and slope data. Both models were calibrated and validated using observed streamflow at the Rabuwabazar station, showing satisfactory with observed streamflow for the respective calibration and validation configurations, with Nash-Sutcliffe Efficiency (NSE) values of 0.79 and 0.75 for SWAT calibration and validation and approximately 0.62 for HEC-HMS. 0.60. Using SWAT and Geographic Information System (GIS) based spatial analysis, 47 potential run-of-river (RoR) hydropower sites were identified, totaling a theoretical hydropower potential of approximately 2992 MW at 40% dependability. This value represents a hydrological and topographic screening estimate rather than technically, economically, environmentally, or socially developable capacity. Furthermore, downscaled and bias-corrected Coupled Model Intercomparison Project Phase 6 (CMIP6) climate projections under SSP1-2.6, SSP2-4.5, and SSP5-8.5 scenarios were integrated with SWAT to assess future runoff and hydropower potential. Results indicate that future flows and power potential are sensitive to emission scenarios, with high-emission pathways yielding increased discharge and potential energy generation. This integrated modeling framework provides a robust approach for sustainable water resource management and climate-resilient hydropower planning in Himalayan basins.

Keywords: Hydrological modelling; Climate change; Streamflow; Climate projection; Climate models; Himalayan watersheds

© 2026 The authors. This is an open access article under the Creative Commons Attribution 4.0 International License (https://creativecommons.org/licenses/by/4.0/).

1. Introduction

Nepal's water resources play a central role in national development, particularly through hydropower generation, agriculture, and domestic supply. With an abundance of rivers originating in the Himalayas, Nepal holds a vast hydropower resource base, with overall potential surpassing 83,000 MW. Of this nearly 43,000 MW is considered technically achievable under current conditions [1]. However, hydropower development is challenged by the complex and heterogeneous nature of Nepal's mountainous watersheds. Steep terrain, large elevation gradients, strong monsoonal seasonality, snow and glacier contributions, and limited hydrometeorological observations create substantial spatial and temporal variability in runoff. Reliable runoff estimation is therefore essential for assessing water availability, hydropower potential, and sustainable water-resource planning [2,3].

The Dudhkoshi River Basin is an important case study because of its substantial hydropower potential and pronounced hydrological variability. The basin is influenced by intense monsoonal rainfall, high-altitude snow and glacier processes, and steep topography, resulting in substantial variation in precipitation, runoff, and river discharge [4]. High-altitude snow and glacier processes, together with steep topography, further complicate runoff estimation in Himalayan catchments [5]. In such a data-constrained and topographically complex basin, uncertainty in hydrological simulation can directly affect hydropower estimates, particularly for run-of-river (RoR) projects that depend strongly on river discharge and its seasonal reliability [6–8].

The Hydrologic Engineering Center–Hydrologic Modeling System (HEC-HMS) is a semi-distributed, event-driven tool developed to analyze how precipitation-runoff processes contribute to runoff in river basins and is widely applied for rainfall–runoff modelling in Nepal [9,10]. In contrast, the Soil and Water Assessment Tool (SWAT) is a continuous, physically based prototype designed to simulate hydrology over long periods by dividing watersheds into Hydrologic Response Units (HRUs), which are defined according to slope characteristics, land use, and soil type. In Nepal, SWAT has been successfully applied in various basins, including Bagmati, Gandaki, as well as Koshi River Basin [11–13]. While HEC-HMS provides design flows and event-based simulations useful in hydropower design, SWAT offers the capability to evaluate long-term flow variability under changing land use and climatic conditions [13]. By comparing the output of both models, decision-makers can gain a more holistic understanding related to the water availability and power generation feasibility. Furthermore, Geographic Information System (GIS)-based spatial analysis and climate change scenarios are incorporated to evaluate present and future hydropower potential, providing insight for climate-resilient and sustainable energy planning in the Dudhkoshi River Basin [14].

Climate change introduces additional uncertainty because changes in temperature and precipitation may alter the magnitude, seasonality, and reliability of future river flows. Integrating hydrological models with downscaled and bias-corrected Coupled Model Intercomparison Project Phase 6 (CMIP6) projections under different Shared Socioeconomic Pathways (SSPs) provides a framework for assessing future runoff and hydropower potential [15]. This is particularly important in Himalayan basins, where changes in precipitation and temperature may also influence snow and glacier processes [5,16].

Although hydrological models have been widely applied in Nepal, limited studies have integrated comparative HEC-HMS and SWAT modeling, spatial RoR hydropower assessment, and climate-change projections in the Dudhkoshi River Basin. Therefore, this study compares HEC-HMS and SWAT for runoff simulation, assesses hydropower potential using SWAT and GIS-based spatial analysis, identifies potential RoR hydropower sites, and evaluates future changes in runoff and hydropower potential under SSP1-2.6, SSP2-4.5, and SSP5-8.5 scenarios. The integrated framework provides a basis for evaluating model-related uncertainty and supporting climate-informed hydropower and water-resource planning in a data-constrained Himalayan basin.

The study is subject to limitations related to the availability and quality of observed data, particularly in the high-elevation areas, and uncertainties in representing complex mountainous hydrological processes, including snow and glacier melt. Additional uncertainties arise from climate models, downscaling, bias correction, and emission scenarios. The hydropower assessment is primarily based on simulated hydrological and topographic characteristics and therefore represents a preliminary estimate of hydropower potential rather than a detailed feasibility assessment. Economic, environmental, social, and detailed engineering factors were not explicitly considered [17].

The remainder of this paper is organized as follows. Section 2 reviews previous studies related to hydrological modelling, climate change impacts on streamflow, and hydropower potential assessment. Section 3 describes the study area, datasets, models, software, and methods used for runoff simulation, hydropower site identification, and climate change assessment. Section 4 presents and discusses the results of HEC-HMS and SWAT model performance, hydropower potential assessment, and future streamflow and hydropower projections under different climate scenarios. Finally, Section 5 summarizes the main findings of the study, discusses the major implications and limitations, and provides recommendations for future research.

2. Literature Review

Hydrological modeling is a fundamental tool for evaluating water availability, managing runoff, and identifying hydropower opportunities, particularly in mountainous countries like Nepal that face complex climatic and topographic challenges [18]. Due to the country's rugged terrain, highly variable precipitation patterns, and increasing vulnerability to climate change, robust hydrological modeling approaches are essential for sustainable planning. In this context, two widely used models, HEC-HMS and SWAT, have gained prominence for simulating runoff, assessing water balance, and supporting water-energy planning [19]. This study uses both models for runoff estimation, and SWAT is also used for hydropower site identification and for evaluating climate change impacts using CMIP6-based scenarios integrated with spatial technology [4,20].

2.1. Runoff Estimation Using HEC-HMS and SWAT

Accurate runoff estimation plays a key role in sustainable water-resource governance and hydropower development, especially in mountainous countries like Nepal. HEC-HMS has been applied to model runoff in the West Rapti River Basin and has been found suitable for rainfall–runoff analysis [9]. Similarly, HEC-HMS was evaluated for the Karnali River Basin using TRMM satellite rainfall data, highlighting its applicability in a data-scarce mountainous catchment [21]. The use of HEC-HMS for hydrograph estimation has also been discussed in methodological studies [12,13].

SWAT, a semi-distributed, process-based model, is suited to long-term watershed simulation and can simulate hydrology as well as sediment and nutrient processes. Applications in Nepal include runoff and hydropower assessment in the Marsyangdi River Basin [22] and integrated GIS–SWAT assessment in the Sunkoshi River Basin [12]. SWAT has also been used to assess sediment yield in the Budhi Gandaki Basin [23]. Comparative research examining HEC-HMS and LSTM illustrates the broader range of approaches used for runoff simulation in mountainous Nepal [20,24].

2.2. Hydropower Potential Site Identification Using SWAT and Spatial Technology

Nepal's hydropower potential remains largely untapped due to limited site identification and technical assessments. The integration of hydrological modeling (like SWAT) with GIS-based spatial analysis has enhanced the ability to identify feasible RoR hydropower sites. Ref. [22] conducted a detailed study combining SWAT modeling and GIS techniques in the Marsyangdi River Basin, identifying 79 potential

RoR sites based on flow accumulation and elevation gradient. Their method involved overlay analysis and thresholding of stream power index values to delineate optimal hydropower locations.

Similarly, Bhattarai et al. [11] utilized a spatially integrated approach with SWAT and GIS in the Sunkoshi Basin, identifying 36 candidate sites for RoR hydropower and estimated a total hydropower potential of 371.30 MW at a 40% probability of exceedance. Their study emphasized that hydrological modeling alone is insufficient; spatial analysis is crucial for site prioritization based on terrain, accessibility, and land use. Bista et al. [8] focused on the outcome of different digital elevation models (DEMs) on hydropower site identification in the West Rapti Basin. They demonstrated how topographic inputs influence gradient and flow path analysis, affecting the accuracy of hydropower potential estimates [25].

2.3. Climate Change Impact Assessment Using SWAT and CMIP6 Scenarios

Climate change is projected to alter rainfall patterns and snowmelt regimes across the Himalayas, directly affecting runoff and hydropower production [5]. To assess future impacts, recent studies have increasingly applied SWAT together with climate projections to assess future streamflow changes in Himalayan and other mountainous river basins. An investigation on the Tamor River Basin by ref. [6] applied SWAT with CMIP6 climate projections based on the SSP2-4.5 and SSP5-8.5 scenarios. Their findings indicated a seasonal shift in peak flows, with higher discharge in monsoon months and declining pre-monsoon flows that could affect hydropower generation reliability. Though several studies in Nepal have used CMIP5 datasets, recent adoption of CMIP6 has improved resolution and reliability. Incorporating bias-corrected GCM outputs with SWAT enables better simulation of future runoff scenarios, which is crucial for designing resilient hydropower systems. Changes in river flow have also been linked to hydropower production in the Kulekhani project [16]. Although uncertainties remain due to model assumptions, emission pathways, and downscaling techniques, assessing multiple climate scenario approaches can support more robust planning [3].

Recent studies further underline the need to consider climate-input uncertainty, seasonal flow variability, and the translation of projected runoff into hydropower outcomes. Nakhaei et al. [26] assessed climate-change effects on river streamflow under alternative pathways, while Ghazikhani et al. [27] examined machine-learning post-processing of climate precipitation. Kumar et al. [28] investigated hydrological and environmental-flow dynamics in a central Himalayan basin, and Pandey et al. [29] assessed climate-related hydrological alteration in the Seti watershed. Pradhananga et al. [30] highlighted the implications of changing seasonal flows for water, energy, and agriculture. At the broader regional scale, integrated climate–hydrology–energy assessments have been applied to Himalayan basins [31], while recent studies of eastern Nepal and the Khimti basin also demonstrate the importance of evaluating hydropower under changing hydroclimatic conditions [32]. Together, these studies support the use of multiple climate scenarios and basin-specific hydrological analysis in the present study.

2.4. Research Gap and Study Contribution

Previous studies have widely applied HEC-HMS, SWAT, and GIS-based approaches for runoff simulation and hydropower assessment in Nepal [13,19]. Recent studies have also used climate projections to examine future changes in streamflow. However, these approaches have generally been applied separately, and limited attention has been given to integrating comparative hydrological modeling, spatial hydropower site identification, and future climate assessment within the Dudhkoshi River Basin. There is also limited assessment of how different hydrological models represent runoff and how future changes in streamflow may affect run-of-river hydropower potential.

This study addresses these gaps through an integrated assessment of runoff, hydropower potential, and climate change. HEC-HMS and SWAT are compared using observed streamflow data, while the calibrated

SWAT model is integrated with spatial analysis to identify potential run-of-river (RoR) hydropower sites based on drainage area, elevation, hydraulic head, and flow availability. In addition, multiple climate models under SSP1-2.6, SSP2-4.5, and SSP5-8.5 are incorporated into SWAT to assess future discharge and hydropower potential. The identified potential sites are also compared with existing licensed hydropower projects, providing a broader basis for hydropower planning and climate-informed water-resource management in the Dudhkoshi River Basin.

The comparison in Table 1 shows that the novelty of the present study is not the use of any single model or GIS method in isolation, but their combined application to the Dudhkoshi River Basin. The contribution is basin-specific and should be interpreted as an integrated hydrological and topographic screening assessment, not as a full engineering feasibility study.

Table 1. Summary of previous studies, research gaps, and contributions of the present study.

Study/Approach	Main Focus or Contribution	Limitation Relative to This Study	Contribution of This Study
HEC-HMS applications in Nepal [9,21]	Rainfall–runoff simulation in data-constrained catchments.	Generally focused on runoff simulation rather than the combined workflow used here.	Compares HEC-HMS with SWAT at Rabuwabazar and distinguishes event-based from continuous simulation.
SWAT–GIS hydropower assessment in Marsyangdi and Sunkoshi [12,22,27]	Uses simulated discharge and terrain attributes to identify candidate run-of-river sites.	Provides basin-specific site screening; does not establish the exact combined assessment for Dudhkoshi.	Identifies 49 candidate sites using the study's screening criteria and estimates theoretical potential from Q40 and gross head.
Climate-change streamflow studies [6,26]	Evaluates climate-driven changes in streamflow under future scenarios.	Results are basin- and model-specific and do not directly establish Dudhkoshi site-level hydropower response.	Applies three CMIP6 GCMs and three SSPs to SWAT and compares future Q40/Q50 discharge and associated power estimates.
Climate precipitation post-processing [27]	Examines a machine-learning post-processing method for climate precipitation forecasts.	Focuses on precipitation post-processing rather than the integrated Dudhkoshi runoff–hydropower workflow.	Highlights the importance of assessing climate-input uncertainty in impact assessments.
Present study	Integrates model comparison, spatial site screening, and climate-scenario analysis for Dudhkoshi.	Subject to observed-data, cryosphere representation, climate-model, and preliminary-screening limitations.	Combines HEC-HMS and SWAT evaluation, GIS-based RoR site identification, and multi-GCM/SSP projections.

3. Materials and Methods

The methodology of this study follows a sequential framework linking basin characterization, data preparation, hydrological modeling, model evaluation, hydropower assessment, and climate change analysis. First, the Dudhkoshi River Basin is described in terms of its geographic, topographic, climatic, and hydrological characteristics to establish the physical context of the study. Second, the hydrometeorological and spatial datasets, together with the software and tools used in the analysis, are presented. These datasets are then processed and prepared as inputs for the hydrological models. The HEC-HMS and SWAT models are subsequently configured to simulate basin runoff, followed by calibration and validation against observed streamflow to evaluate their performance. The validated SWAT model is then linked with spatial analysis to identify potential RoR hydropower sites and estimate their hydropower potential. Finally, climate projections under different SSP scenarios are incorporated into the hydrological modeling framework to assess potential changes in future runoff and hydropower potential. Thus, each subsection builds upon the preceding one, progressing from basin characterization and data preparation to runoff simulation, model evaluation, hydropower assessment, and climate change impact analysis.

3.1. Study Area

The study was carried out in the Dudhkoshi river basin (Sub-Basin of Koshi) situated in Eastern Nepal. It is situated between 27°56′05″ N to 27°08′58″ N latitudes and 86°42′34″ E to 86°26′00″ E longitudes. The Sub-basin covers a total area of approximately 3712.00 sq. km. The topographic height of the basin varies between 8848 masl (Mount Everest) to 465 masl (Rabuwa Bazar, Khotang Gauging Station) and average elevation of 3800 masl.

The annual precipitation varies from about 1000 mm in the lower areas to over 3000 mm in the upper regions. This variability is largely under the influence of the Asian monsoon system and the snowmelt contribution from the Himalayan glaciers. These factors make the basin a key area for studying the interaction between rainfall and snowmelt in hydrological modeling. The study area is shown in Figure 1.

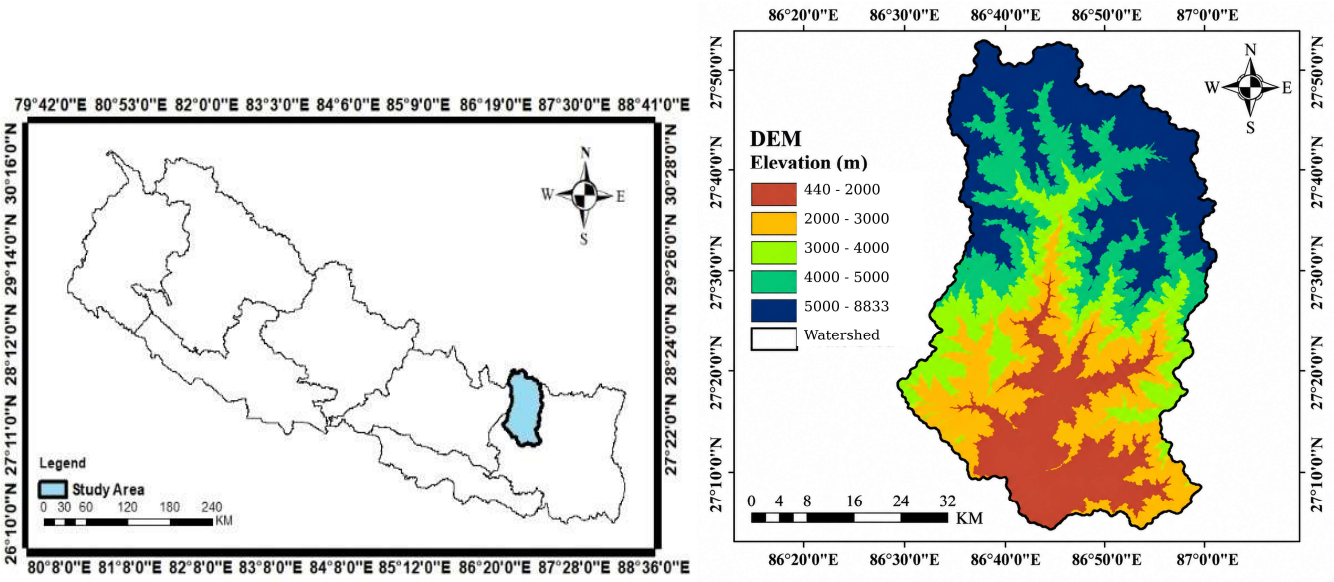


Figure 1. Location of Study Area.

3.2. Data and Tools Used

3.2.1. Hydrometeorological Data

Hydrometeorological data, including rainfall, temperature, and discharge data from approximately ten monitoring stations located within and neighboring the Dudhkoshi River Basin watershed were selected. Daily data records were obtained for these stations spanning a period of 35 years, from 1985 to 2020. The Stations are Presented in Table 2.

Table 2. List of Hydrometeorological Stations with Coordinates.

Station ID	Station Name	Latitude (m)	Longitude (m)	Elevation (m)	Purpose
670	Rabuwabazar	27.26871	86.65924	470.64	Discharge
1206	Okhaldhunga	27.30812	86.50423	1728.67	Rainfall and Temperature
1204	Aiselukharka	27.35979	86.74866	2063.03	Rainfall
1202	Chaurikharka	27.69653	86.71670	2639.48	Rainfall
1222	Diktel	27.21252	86.79189	1613.78	Rainfall and Temperature
1211	Khotang	27.55564	86.37233	1622.58	Rainfall
1207	Manebhanjyang	27.21473	86.44436	1534.03	Rainfall
1203	Pekarnas	27.44322	86.56857	1942.22	Rainfall
1219	Salleri	27.50512	86.58621	2383.85	Rainfall and Temperature
1224	Siruwa	27.55564	86.37233	1622.58	Rainfall

3.2.2. Land Use and Soil Data

Figure 2a represents the watershed boundary, drainage network, outlet at Rabuwabazar, and the locations of nearby rainfall stations used to collect precipitation data for hydrological modelling whereas Figure 2b. shows the stream network of the watershed, classified into different stream orders based on the branching pattern. The watershed includes glaciers, snow, forest, cropland, built-up areas, grassland, and bare rock/soil, which is shown in Figure 2c. The presence of glaciers and snow-covered areas in the north, and more vegetated/agricultural areas in the south, suggests significant elevation gradients typical of Himalayan catchments. Spatial variability in land use, soil type, and terrain is evident—a key factor for selecting an appropriate hydrological model. In this study, land use data for the Dudhkoshi River Basin were derived from recent satellite imagery (e.g., Landsat 8) and classified using GIS techniques to generate input layers for both HEC-HMS a well as SWAT models. Three distinct types of soil were obtained inside the Dudhkoshi Watershed using the Soil and Terrain Digital Database (SOTER) soil map, where Ultisols and Alfisols was seen to be dominant as shown in Figure 2d.

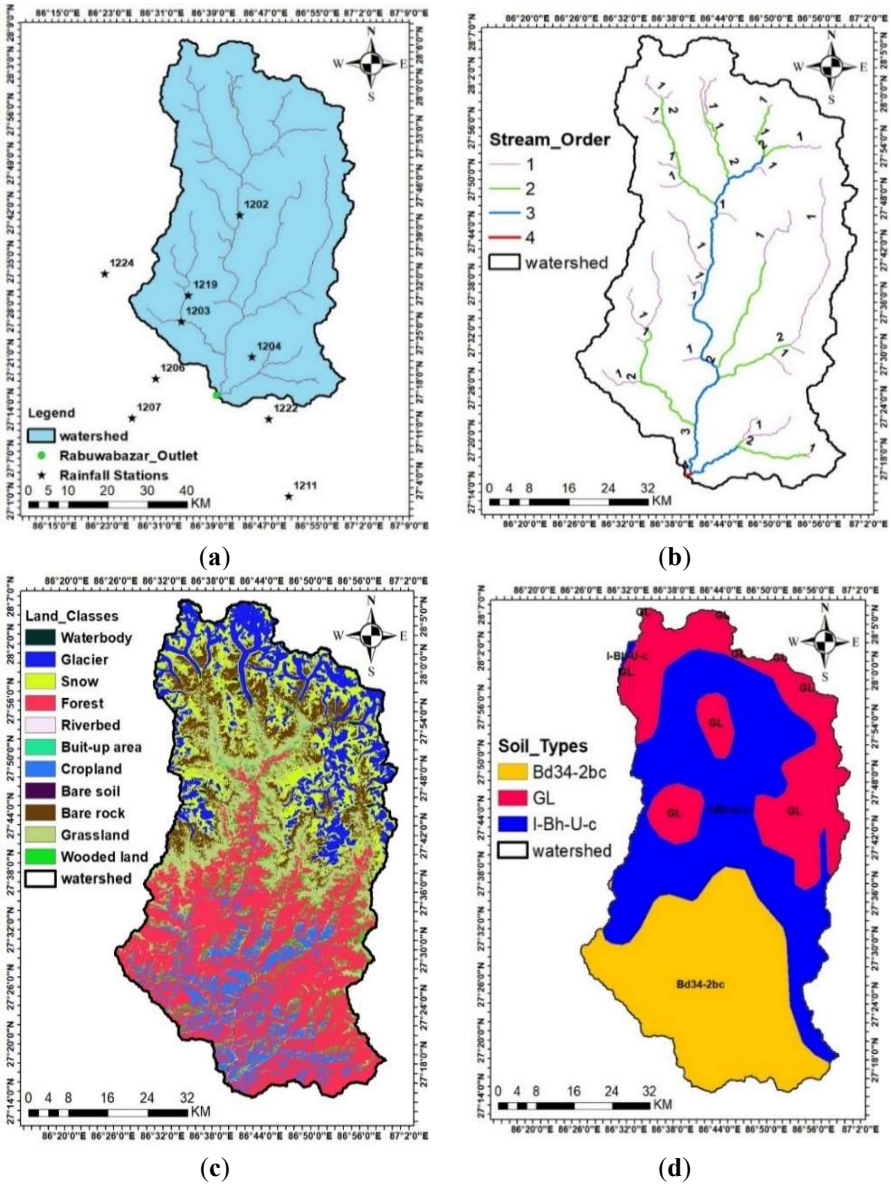


Figure 2. (**a**) Hydrometeorological Station, (**b**) Stream Order in Watershed, (**c**) LULC Map and (**d**) Soil Map.

3.2.3. Climate Data

Future climate data were obtained under the CMIP6 framework using daily outputs from a trio of General Circulation Models (GCMs). Three SSPs were considered: Low-Emission scenario (SSP1-2.6), intermediate scenario (SSP2-4.5), and high-emission scenario (SSP5-8.5). Daily meteorological data on precipitation and temperature from these models were served as inputs for the SWAT model to simulate runoff trends. The simulations were conducted for two-separate horizons-near term future (2021–2050) and distant future (2051–2080)-to examine the influence of climate change on streamflow patterns in the Dudhkoshi River catchment. The CMIP6 scenario framework follows the Scenario Model Intercomparison Project (ScenarioMIP) design [33].

3.2.4. Software Used

ArcGIS Desktop version 10.5, developed by Esri, California, USA is a robust GIS software that was employed for watershed delineation, extraction of topographic parameters, and preparation of spatially referenced data DEM, soil layers, and land use patterns for hydrological modeling in both HEC-HMS and Arc SWAT. For this study, HEC-HMS version 4.12 was employed for runoff simulation within the Dudhkoshi River Basin. Arc-SWAT 2012(version 2012.10_5.24), a GIS-based tool, was used to integrate spatial datasets such as DEM, land cover, and soil layers, facilitating watershed delineation and preparation of inputs for hydrological modeling. The Soil and Water Assessment Tool-Calibration and Uncertainty Programs (SWAT-CUP 2012) version 5.1.6 developed by the Swiss Federal Institute of Aquatic Science and technology was used to calibrate, validate, and perform sensitivity and uncertainty analyses of SWAT model outputs.

3.3. Methodology

3.3.1. HEC-HMS Model Setup

The process begins with defining the basin geometry, including boundaries, sub basins, and channel networks. Topographic data, such as DEMs, are crucial for delineating these features, as shown in Figure 3. Next, meteorological data, including rainfall and temperature records, are incorporated to drive the rainfall-runoff processes. These data are used to drive the rainfall-runoff dynamics. The model parameters represent watershed characteristics such as soil type, land cover, and channel roughness. These parameters are calibrated against observed streamflow. After calibration, the model was used to simulate runoff and evaluate its performance against observed streamflow. The model setup and simulation procedures are consistent with the HEC-HMS technical documentation [34].

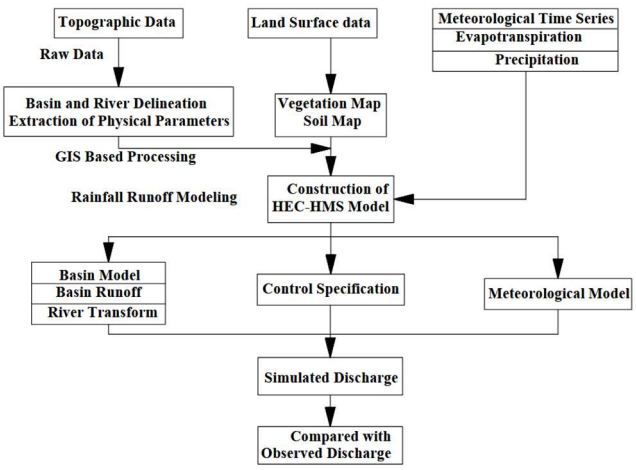


Figure 3. Flow Diagram of Methodology Through HEC-HMS.

Figure 3 summarizes the sequence of HEC-HMS model preparation, meteorological input, parameterization, calibration, and runoff simulation. This workflow clarifies how the spatial basin representation and observed streamflow are linked. Because the HEC-HMS setup is event-oriented, interpret its performance in relation to the selected rainfall–runoff configuration and available observations rather than assuming it is directly equivalent to the continuous SWAT simulation.

3.3.2. Arc-Swat Model Setup

Figure 4 shows the SWAT workflow from watershed delineation and HRU generation to weather-data preparation, calibration, and validation. The model uses land use, soil, slope, and meteorological inputs to represent spatial variability across the basin. The calibration and validation periods are separate, allowing the model's ability to reproduce observed discharge to be assessed beyond the calibration period.

In this study, the entire watershed was first delineated into 23 sub-watersheds during the model setup. These sub-basins were then subdivided into 813 HRUs. The model was calibrated for the period from 1 January 1985 to 31 December 2010 (25 years) and validated from 1 January 2011 to 31 December 2020 (10 years). A warm-up period of four years (1 January 1985 to 31 December 1988) was included to equilibrate various water storages within the model. Observed streamflow data from the 670 Rabuwabazar hydrological station was used for model development. Sensitivity analysis was conducted using a manual calibration approach. SWAT-CUP was then used to identify the most sensitive parameters affecting streamflow. In the developed SWAT model, surface runoff was estimated using the Soil Conservation Service Curve Number (SCS-CN) method, while potential evapotranspiration was calculated with the Hargreaves method. The DEM of the Dudhkoshi watershed was initially delineated into sub-watersheds using the SWAT watershed delineation tool. Reclassified land use and soil maps were then incorporated as model inputs, followed by the addition of weather data. Finally, observed streamflow at the 670 Rabuwabazar station was used to calibrate the model. SWAT model configuration and calibration practice are described in the SWAT methodological literature [35,36].

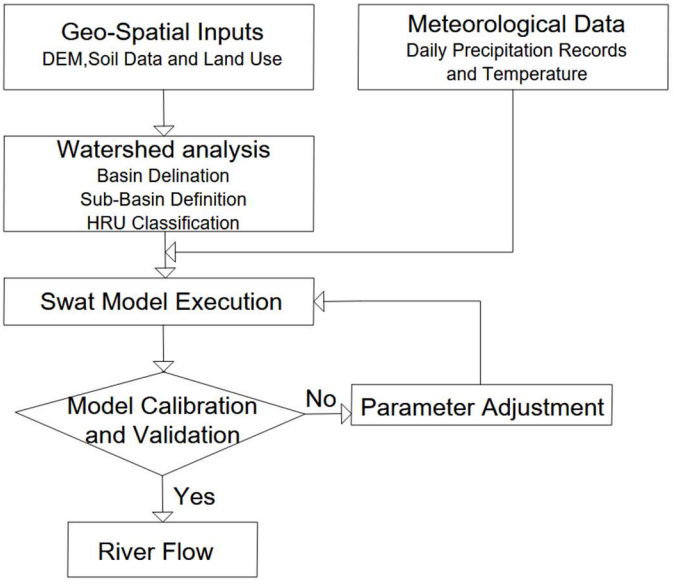


Figure 4. Flowchart of Hydrological Modelling in SWAT.

3.3.3. Arc-Swat Model Setup for Hydropower Potential

A DEM was utilized to derive flow direction and discharge accumulation. A minimum contributing area threshold of 500 hectares was applied for watershed delineation. After delineation, the channel network, channel order, and watershed outlet were identified, and the corresponding sub-basins were generated. The

delineated watershed was then exported from the GIS environment and imported into Google Earth. From the initially defined outlet of each sub-basin, a point 2000 m downstream was identified using the ruler tool in Google Earth. These downstream points were considered potential intake locations for hydropower development. Figure 5 links GIS-derived stream and elevation information with SWAT discharge estimates to screen potential hydropower sites. Neither discharge nor elevation difference alone is sufficient to estimate theoretical hydropower potential; both flow availability and gross head contribute to the calculation. The resulting sites remain candidates for further investigation rather than confirmed feasible projects.

Subsequently, locations for potential powerhouse sites were determined. The corresponding KML file from Google Earth was imported back into ArcGIS to calculate the elevation difference (head) between intake and powerhouse locations. Only sites with a head greater than 40 m and an elevation below 3000 m above sea level (masl) were considered viable. Points located in areas with significant river meandering, dense building infrastructure, or designated buffer zones were excluded from further analysis. The remaining suitable intake points were applied as inputs in the SWAT model for predicting river discharge. For each intake location, a corresponding sub-basin was created in SWAT, and flow simulations were performed. Monthly discharge data for the period 1989–2020 were averaged for each site. The Period (1985–1988) was considered the warm up period. The required design discharge Q40 (40% exceedance flow) was then estimated using flow duration curves derived from probability of exceedance analysis.

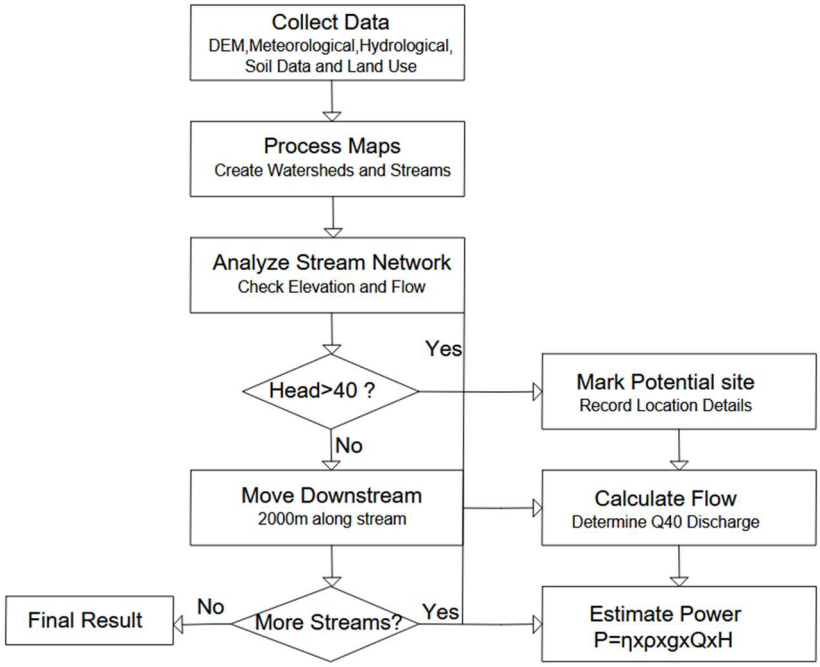


Figure 5. Flowchart of Methodology of calculating Hydropower Potential.

3.3.4. Criteria for Identification of Site

The identification of suitable hydropower sites was initiated at the upstream sections of the river network and proceeded downstream, ensuring a minimum spacing of 2 km between consecutive locations. As the study focused on small- to medium-scale hydropower development, a set of criteria was applied to screen potential RoR project sites: GIS-based screening of run-of-river hydropower locations has also been demonstrated in Nepalese watersheds [37].

- Streams of all orders with a minimum drainage area threshold of 5 km^2 were considered for potential RoR hydropower development.
- For efficient system design, the distance between the intake (weir) and powerhouse was limited to 2 km and 5 km to ensure adequate head while limiting penstock length.

- A minimum head of 40 m was required for each site to ensure power generation feasibility. Additional screening excluded location near settlements, sharp river bends, and hazard-prone areas.

The site-screening procedure should be regarded as a preliminary hydrological and topographic assessment rather than a full engineering feasibility study. The spatial thresholds were adopted as study-specific GIS screening criteria, informed by the characteristics of the basin and previous GIS-based hydropower assessments, rather than as universal engineering standards. A minimum head of 40 m was used to identify sites with a sufficient hydraulic gradient, while the 2 km intake-to-powerhouse spacing criterion was applied to identify reaches with adequate elevation differences without assuming excessively long conveyance distances. The 3000 m elevation threshold was used to exclude high-elevation areas where snow and glacier conditions, steep terrain, accessibility, and construction constraints may be significant, and the minimum drainage area of 5 km^2 was applied to avoid very small headwater reaches with limited simulated discharge.

The estimated hydropower capacity was primarily based on simulated Q40 discharge and elevation-derived gross head and therefore represents theoretical or gross hydropower potential for screening purposes, rather than directly developable installed capacity. Factors such as geological and geotechnical conditions, environmental-flow requirements, sediment management, access and construction requirements, transmission connectivity, land acquisition, project costs and economics, and potential social and ecological impacts were not explicitly assessed. Consequently, detailed site-specific engineering, environmental, economic, and social investigations would be required before considering any site for actual project development.

3.3.5. CMIP6 Model Setup for Climate Change Scenario in Hydropower Potential

Climate data were obtained from CMIP6. These datasets from Global Climate Models (GCMs) were downscaled and bias-corrected to improve their applicability to the study basin. The corrected data were then formatted as input for the SWAT simulation model. The SWAT hydrological modeling tool was configured for the Dudhkoshi Basin, followed by calibration and validation over a 35-year period. The series of steps are shown in Figure 6. Sensitive analysis was performed to identify the hydrological parameters that most strongly influenced streamflow. The SWAT model outputs were analyzed to access:

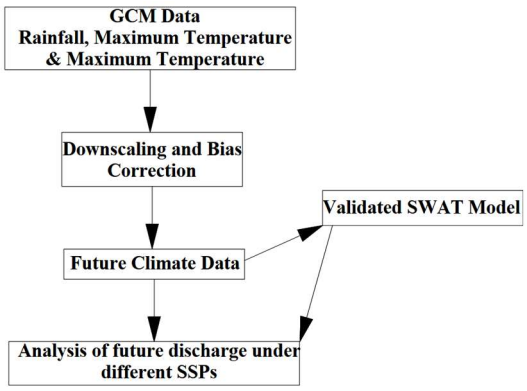


Figure 6. Flowchart of Methodology of climate change (CMIP6).

Figure 6 summarizes the climate-impact workflow, in which downscaled and bias-corrected GCM inputs are supplied to the calibrated SWAT model. The use of multiple GCMs and SSPs helps characterize a range of possible future responses rather than a single forecast. Interpretation remains conditional on the climate data, bias-correction procedure, and hydrological-model assumptions.

- Discharge trends under each climate condition, including SSP1-2.6, SSP2-4.5, and SSP5-8.5.
- Rainfall distribution across future time intervals, namely the near future (2021–2050) and distant future (2071–2100).

4. Result and Discussions

4.1. Results

4.1.1. HEC-HMS Calibration and Validation

Calibration and validation at the Rabuwabazar (670) hydrological station show that the HEC-HMS model performed moderately well, with NSE values of 0.62 and 0.60, respectively, as shown in Figures 7 and 8. The model slightly overestimated streamflow during both periods (PBIAS of 18% during calibration and 20% during validation), indicating a reasonable representation of the basin's hydrological response at the upstream station.

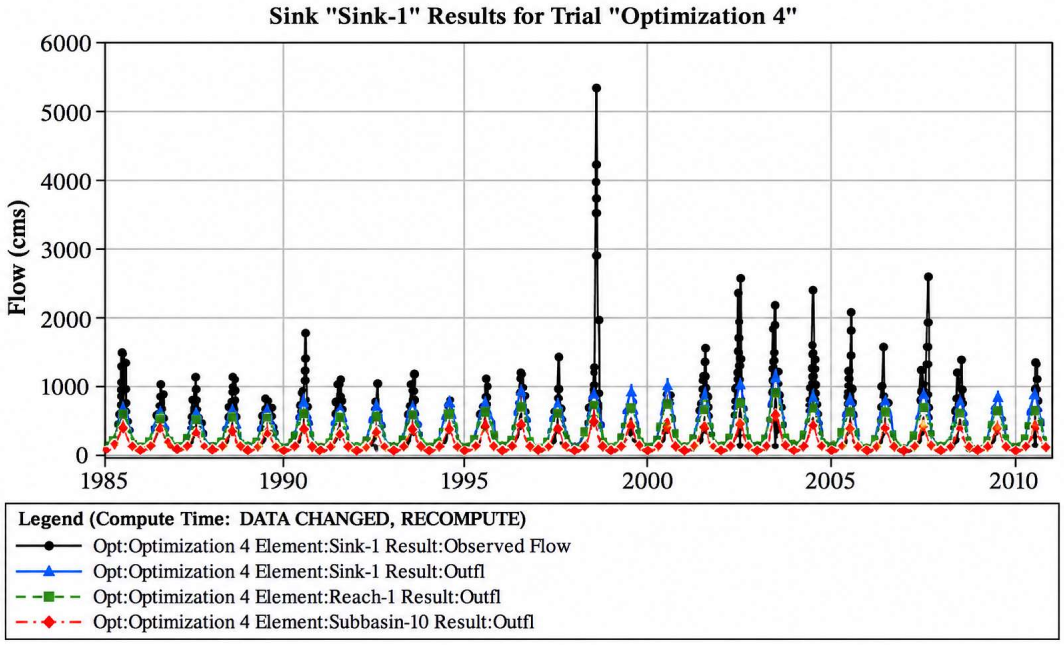


Figure 7. Calibration Through HEC-HMS.

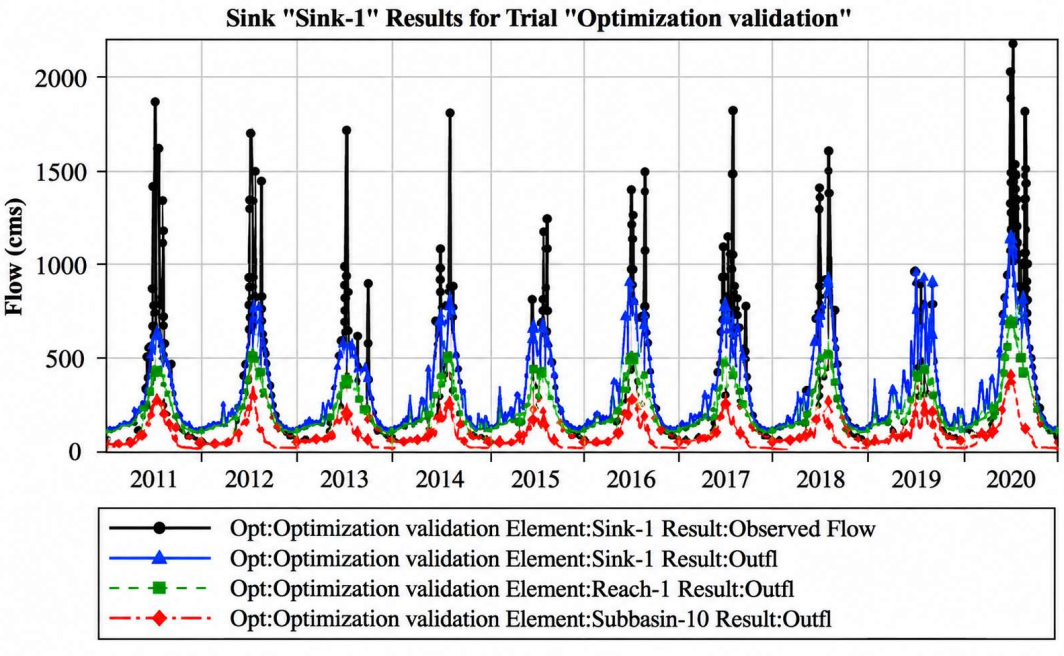


Figure 8. Validation Through HEC-HMS.

4.1.2. Arc-Swat Calibration and Validation

The predictive performance of the ARC SWAT model was analyzed using standard statistical indicators during the calibration and validation phases. The key calibration factors assessed include the Nash-Sutcliffe Efficiency (NSE), P-factor, and R-factor as reported in Table 3. The evaluation follows established watershed-model performance guidance [36,38], with NSE defined by Nash and Sutcliffe [37].

Table 3. Indicator parameters.

Indicator Parameters	Calibration	Validation
NSE	0.79	0.75
P-Factor	0.81	0.6
R-factor	0.46	0.4

Table 3 provides a comparison of the SWAT calibration and validation indicators. NSE declines from 0.79 during calibration to 0.75 during validation, while the P-factor decreases from 0.81 to 0.60 and the R-factor from 0.46 to 0.40. The NSE values indicate that the model retains useful predictive performance in the validation period; the lower validation P-factor also indicates that uncertainty-band coverage is less complete than during calibration. These indicators should therefore be considered together rather than using NSE alone. The evaluation follows established watershed-model performance guidance [36,39], with NSE defined by Nash and Sutcliffe [40].

The best-fitted parameter during calibration were used during model validation. The best-fitted values after five iterative calibration cycles consisting of 800 simulations are presented in Table 4. SWAT model configuration and calibration practice are described in the SWAT methodological literature [38,41].

Table 4. Best Fitted Parameter in SWAT Model.

Parameter Name	Fitted Value	Min_value	Max_value
1: R__CN2.mgt	−0.4901	−2.5076	1.1606
2: V__ALPHA_BF.gw	0.2482	0.0508	0.6742
3: V__GW_DELAY.gw	21.4553	−94.2492	162.872
4: V__GWQMN.gw	2.0581	1.1458	2.3105
5: V__SFTMP.bsn	1.8614	−1.6393	3.2454
6: V__SMTMP.bsn	7.9189	2.5805	9.6984
7: V__SMFMX.bsn	1.4967	0.836	8.7653
8: V__SMFMN.bsn	2.1241	1.6832	3.4468
9: V__TIMP.bsn	1.0087	0.7868	1.6746
10: V__ESCO.hru	0.7559	0.05	1
11: R__SOL_K(..).sol	0.2186	−0.05	2
12: R__SOL_AWC(..).sol	0.1111	0.02	1
13: V__SURLAG.bsn	8.2588	0.05	10
14: V__SLSUBBSN.hru	123.82	10	150
15: V__TLAPS.bsn	−5.8	−4.5	−6
16: V__PLAPS.bsn	280	150	400

Table 4 lists the fitted SWAT parameters and their search ranges. The parameter values show which hydrological processes were adjusted during calibration, including runoff generation, groundwater response, soil-water storage, and snowmelt. Because several snow-related parameters were sensitive, their fitted values should be interpreted with particular caution in this high-elevation basin where direct glacier-melt observations were unavailable.

The Arc SWAT model exhibited robust performance during both calibration and validation, as illustrated in Figures 9 and 10, outperforming HEC-HMS in long-term runoff simulation for the Dudhkoshi

River Basin. The obtained NSE values of 0.79 (calibration) and 0.75 (validation) reflect a strong correspondence between observed and simulated streamflow. Additionally, P-factor values indicate adequate coverage of observed discharge within the predictive uncertainty bands, while low R-factor values confirm a narrow uncertainty range. These results demonstrate the reliability of Arc SWAT for runoff simulation and its applicability in hydropower potential evaluation and climate change impact assessment in the basin.

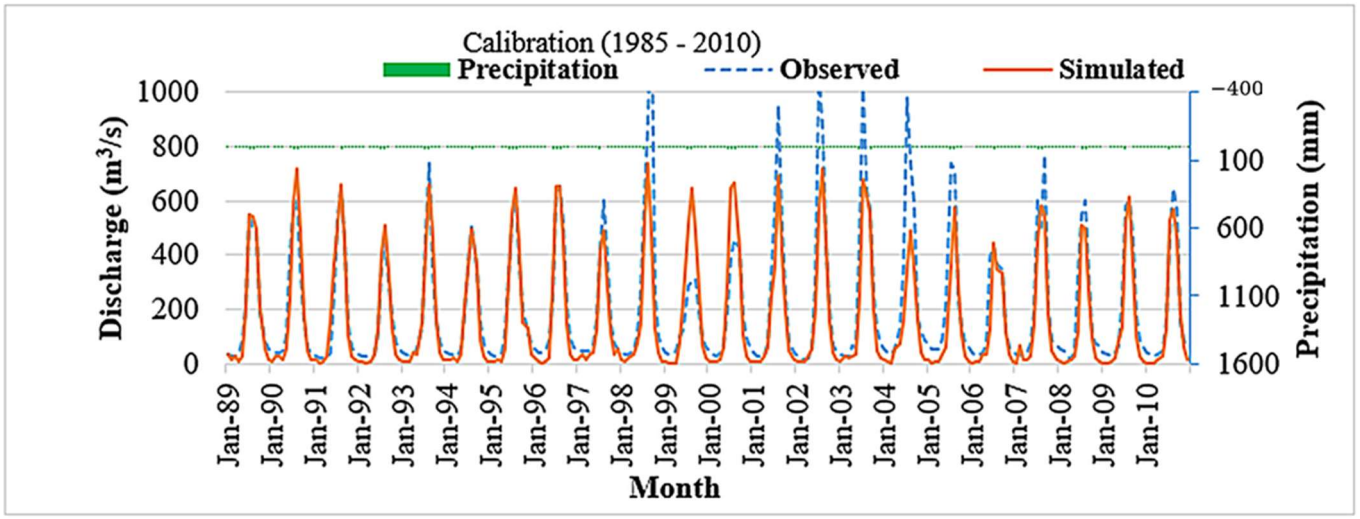


Figure 9. Calibration Through SWAT.

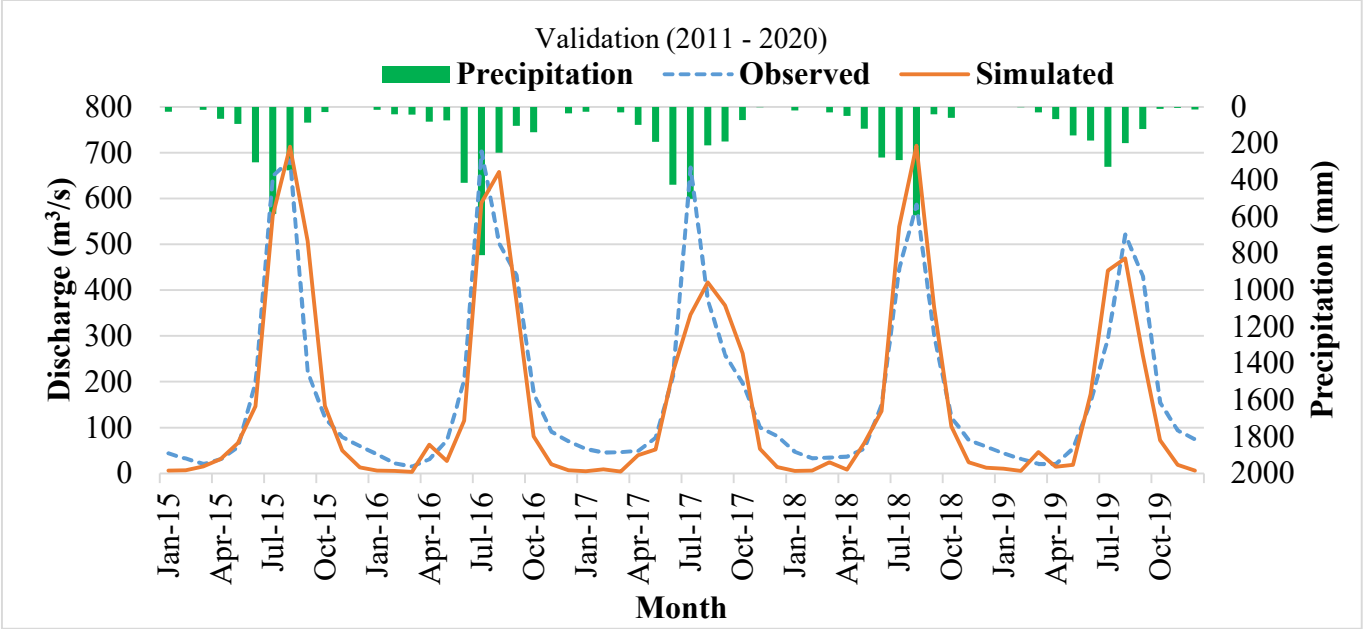


Figure 10 Validation Through SWAT.

Figures 9 and 10 compare temporal patterns of observed and simulated discharge during calibration and validation, respectively. Figures 11 and 12 complement these time-series plots by comparing simulated and observed values directly. Their reported R^2 values (approximately 0.79 for calibration and 0.81 for validation) indicate a strong association, but association alone does not prove unbiased predictions; NSE and bias/error indicators should also inform the overall assessment. Any mismatches can reflect rainfall-input uncertainty, parameter limitations, and processes that are difficult to observe at high elevations.

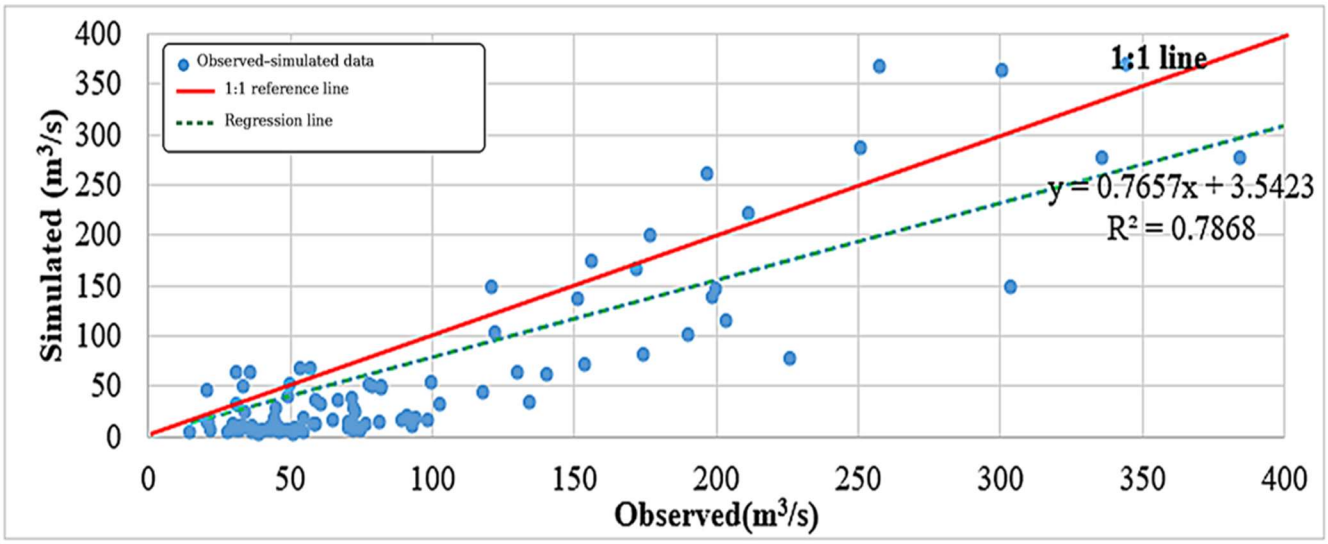


Figure 11. Scatter Plot for Calibration.

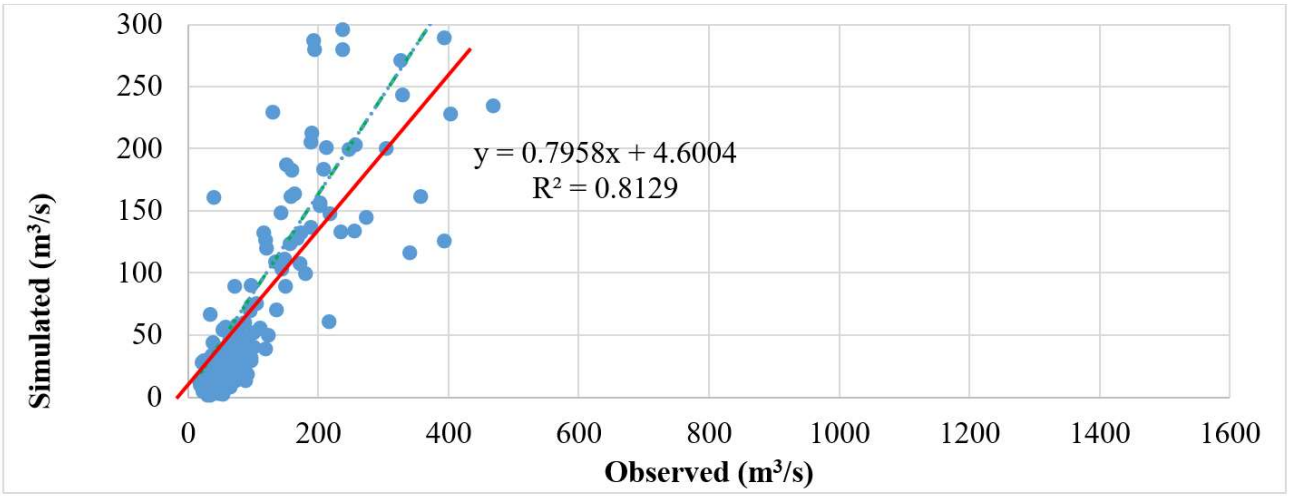


Figure 12. Scatter Plot for Validation.

4.1.3. Sensitive Parameters

Figure 13 presents the parameter-response patterns used to evaluate sensitivity. The sensitivity analysis of the four snowmelt-related SWAT parameters SFTMP, SMTMP, SMFMX, and SMFMN shows that the modeled hydrological response varies across their tested parameter ranges. The variations in SFTMP and SMTMP indicate sensitivity to the temperature thresholds controlling snowfall and snowmelt, while the response to SMFMX and SMFMN demonstrates the influence of maximum and minimum snowmelt rates on simulated runoff. These results provide quantitative evidence that snowmelt parameterization is an important source of uncertainty in runoff simulation for the glacier- and snow-influenced Dudhkoshi River Basin. This analysis is particularly important in the absence of direct *in-situ* glacier melt observations, as it evaluates the sensitivity of the modeled cryosphere-related runoff processes through key snowmelt parameters. Although glacier melt rates themselves could not be directly constrained, the sensitivity analysis demonstrates that uncertainty in snowmelt representation can influence the modeled hydrological response and should therefore be considered when interpreting the subsequent hydropower projections.

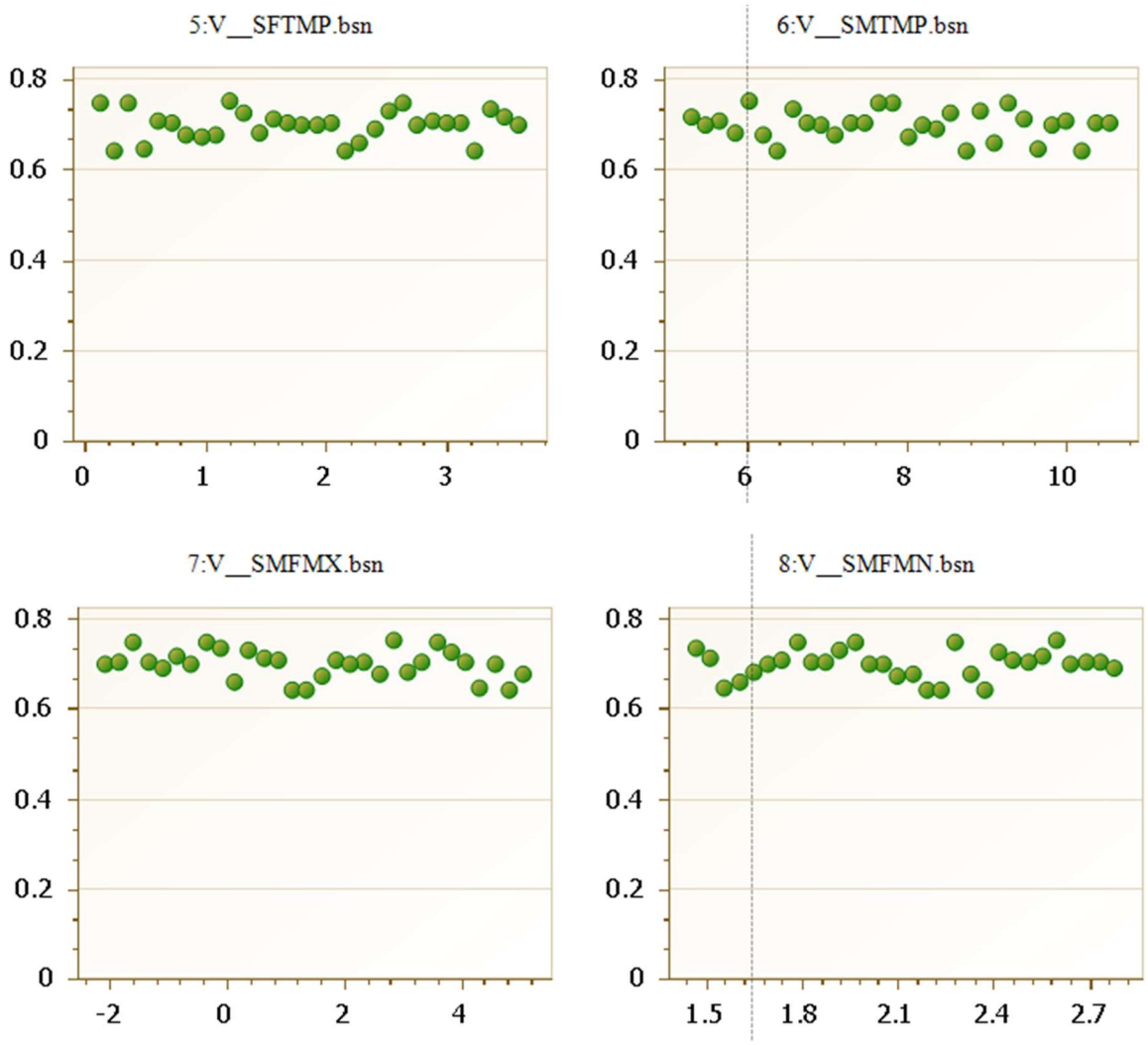
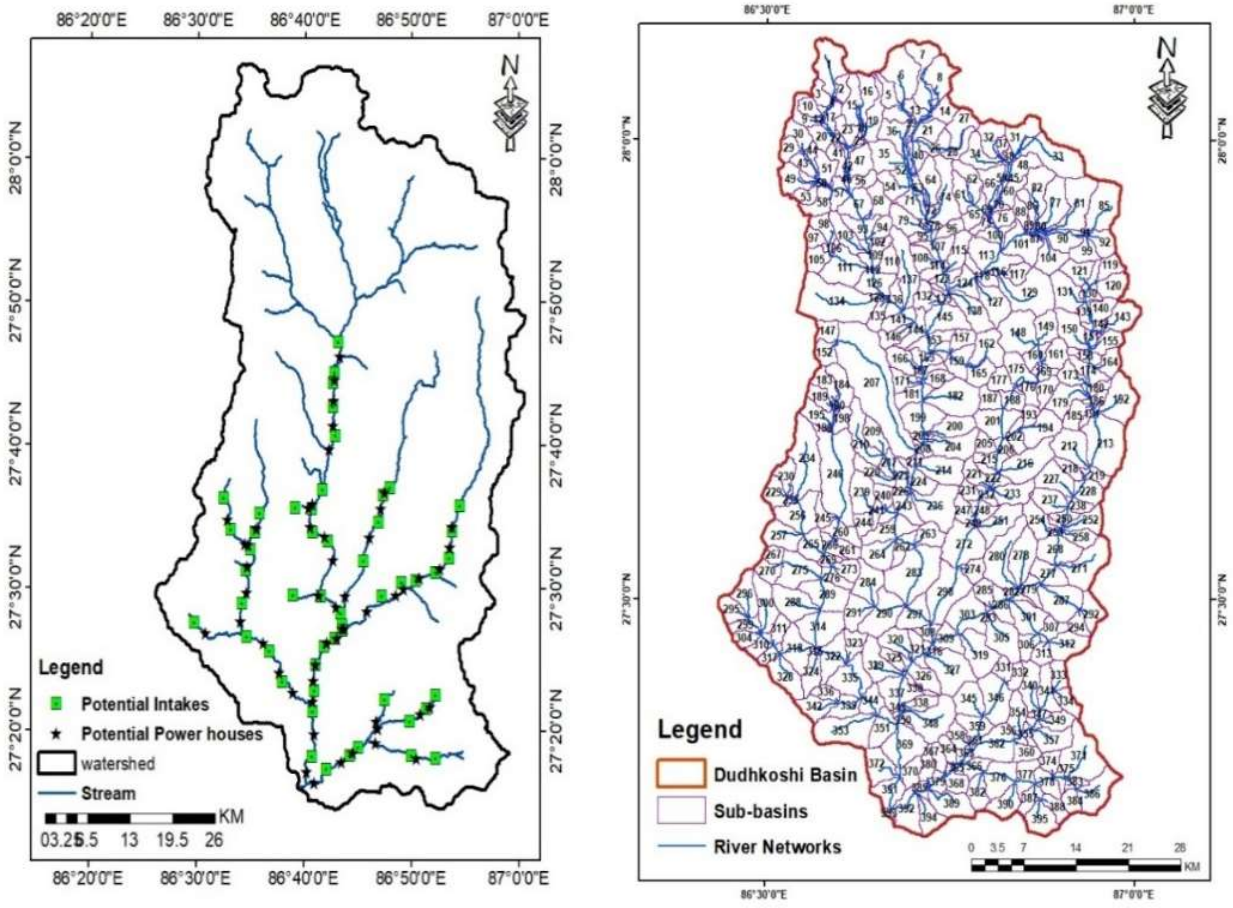


Figure 13. Dotty Plots for sensitive parameter.

4.1.4. Identification of Run-of-River Hydropotential Sites

Figure 14a shows the candidate powerhouse locations, while Figure 14b presents the watershed delineation used for the spatial analysis. The screening process reduced the initial 204 locations to 57 after applying the stated head, drainage-area, and elevation criteria, and then to 47 sites after additional exclusions for meandering and buffer-zone constraints. This stepwise reduction demonstrates why the final site count depends on the explicit GIS thresholds and should not be interpreted as a complete inventory of technically feasible projects.

In total, 204 locations were identified as potential sites. Among the identified locations, 147 sites were discarded as they didn't fulfil the criteria for head, threshold drainage area of 5 km^2 and they lied above the elevation of 3000 m as it is glacier buffer zone. Hydropower sites were identified only within an elevation range of (495–3000) m only. From remaining: 57 potential sites, only 47 sites were considered as they lied in meandering and forest buffer zone. The list of identified potential sites is presented in the appendix at last.



(**a**) (**b**)

Figure 14. (**a**) Potential Powerhouse location, (**b**) Watershed Delineation of our watershed.

4.1.5. SWAT Model

The watershed delineation of the Dudhkoshi watershed was generated in SWAT within an area of 3712 km². Using a threshold area of 5 km^2, 395 sub-basins were delineated based on automatically generated outlets (Figure 14b). To define Hydrologic Response Units (HRUs) within these sub-basins, land use maps, soil maps, and slope data derived from the DEM were utilized. As a result, the SWAT model generated a total of 4822 HRUs across the 395 sub-basins.

4.1.6. Flow Duration Curve for Hydropower Assessment

Figure 15 represents a flow duration curve, which shows the variation of streamflow discharge (in m^3/s) with respect to the percentage of exceedance, indicating how often a particular discharge is equaled or exceeded over time. The curve demonstrates that high discharges (around 600 m^3/s) occur infrequently (below 10% exceedance), while lower discharges dominate most of the time. There is a sharp decline in discharge from 20% to 40% exceedance, beyond which the curve flattens, reflecting more stable, lower flows. Notably, the discharge at Q40 (40% exceedance Discharge) on this curve is approximately 171 m^3/s, meaning this flow is exceeded 40% of the time. This value is commonly used in hydropower planning to estimate available water for energy generation under moderately frequent flow conditions.

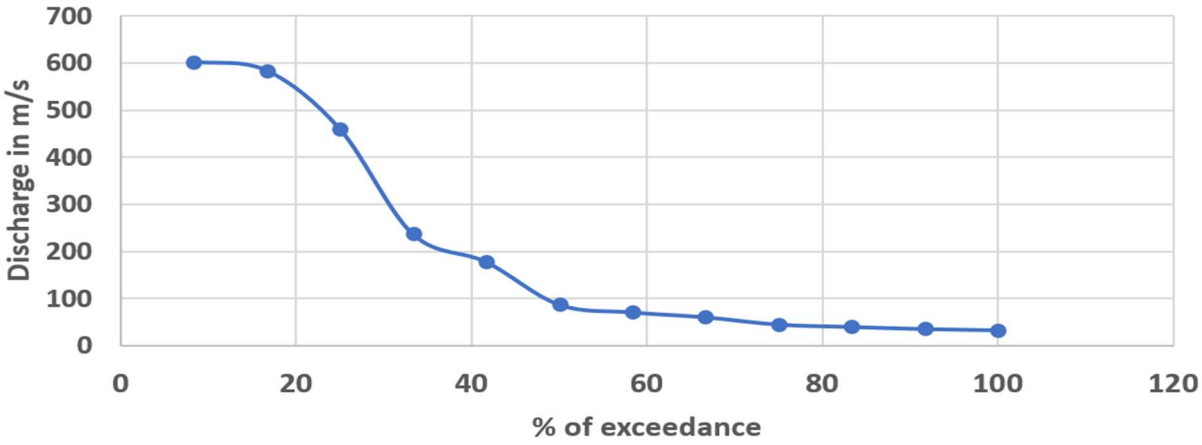


Figure 15. Flow Duration Curve (FDC) for Dudhkoshi River Basin.

The flow-duration curve provides the hydrological basis for the design-flow indicators used later in the study. Q40 is the discharge equaled or exceeded 40% of the time, whereas Q50 is the discharge equaled or exceeded 50% of the time and is the median flow-duration value. These indicators describe flow availability at selected exceedance levels; they are not flood-peak estimates. The approximate Q40 value of 171 m^3/s read from Figure 15 is a reference for the curve shown and should not be confused with the future values in Table 4.

4.1.7. Results from CMIP6 in Integration with SWAT on Discharge

The integration of CMIP6 climate projections with the SWAT hydrological model enabled the simulation of future discharge patterns for the Dudhkoshi Basin under different climate scenarios, which are presented below:

Figure 16 compares projected Q40 and Q50 discharges for the near future (2021–2050) and the far future (2071–2100) under three different emission scenarios SSP1-2.6, SSP2-4.5, and SSP5-8.5, using the EC-Earth3, MPI-ESM1-2-HR, and NorESM2-MM climate models. The projections varied across the models and scenarios, In EC-Earth3, near-future Q40 ranged from 108.7 m^3/s under SSP2-4.5 to 150.0 m^3/s under SSP5-8.5. Far-future Q40 surged under all three scenarios, approaching 202.5 m^3/s under SSP5-8.5. Q50 also escalated across the scenarios, with its highest projected value of 87.0 m^3/s under SSP5-8.5.

MPI-ESM1-2-HR showed an increase in far-future Q40 under all three scenarios, reaching 117.8 m^3/s under SSP5-8.5, while Q50 showed less consistent response where value fluctuated such as the value decreased under SSP1-2.6 but increased under SSP2-4.5 and SSP5-8.5. NorESM2-MM produced a different pattern, with the highest far-future Q40 (145.0 m^3/s) and Q50 (66.6 m^3/s) under SSP1-2.6. Under SSP2-4.5, both values decreased relative to the near future. Under SSP5-8.5, Q40 increased slightly, whereas Q50 declined.

The results from Table 5 demonstrated that projected discharge changes are not consistent across the climate models and emission scenarios. EC-Earth3 and MPI-ESM1-2-HR generally projected higher far-future Q40 values, while NorESM2-MM exhibited a more variable response. This variation should be considered when evaluating future water availability and hydropower potential. Moreover, Q40 and Q50 describe flow-duration characteristics rather than flood peaks; therefore, changes in these indicators alone cannot establish future flood risk, which requires a separate flood-frequency analysis.

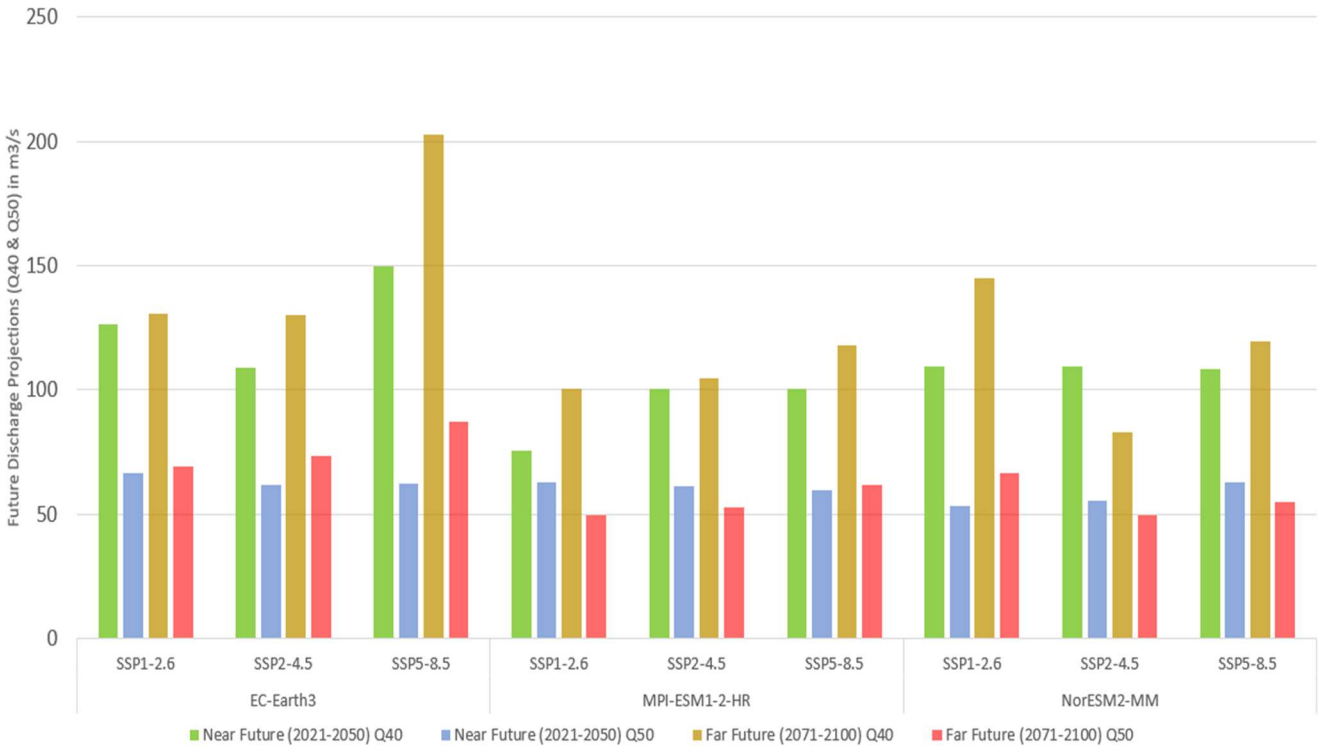


Figure 16. Comparison of projected Q40 and Q50 discharges under three SSP scenarios for EC-Earth3, MPI-ESM1-2-HR, and NorESM2-MM during the near future (2021–2050) and far future (2071–2100).

Table 5. Future Discharge Projections (Q40 & Q50) under SSPs.

GCM	Path	Near Future (2021–2050)		Far Future (2071–2100)	
		Q40	Q50	Q40	Q50
EC-Earth3	SSP1-2.6	126.3	66.7	130.4	69.4
	SSP2-4.5	108.7	61.9	130	73.3
	SSP5-8.5	150	62.5	202.5	87
MPI-ESM1-2-HR	SSP1-2.6	75.6	62.9	100.3	49.7
	SSP2-4.5	100.7	61	104.8	52.9
	SSP5-8.5	100.6	59.5	117.8	62
NorESM2-MM	SSP1-2.6	109.6	53	145	66.6
	SSP2-4.5	109.3	55.4	83	49.6
	SSP5-8.5	108.4	62.7	119.4	55.1

Table 5 shows that the direction and magnitude of change differ across GCMs and SSPs. For EC-Earth3, Q40 increases from 150.0 m^3/s in the near future under SSP5-8.5 to 202.5 m^3/s in the far future, while NorESM2-MM gives a far-future Q40 of 83.0 m^3/s under SSP2-4.5. These contrasting outcomes mean that a single scenario cannot represent the full range of possible future flow conditions. The table values are discharge estimates in m^3/s and should be interpreted as flow-duration indicators, not flood peaks.

4.1.8. Future Predicted Power

Figure 17 depicts the projected hydropower potential of the Dudhkoshi River Basin for SSP1-2.6, SSP2-4.5, and SSP5-8.5 during the near future (2021–2050) and far future (2071–2100). The estimates are based on three climate models, EC-Earth3, MPI-ESM1-2-HR, and NorESM2-MM, and two flow-duration levels, Q40 and Q50. The projections show considerable variation among the models, suggesting that future hydropower potential is sensitive to the climate data and emission scenario used. EC-Earth3 projects near-future Q40 power potential of 1900.7–2623.8 MW, with the maximum under SSP5-8.5. The far-future

estimates rise to 2273.5–3540.8 MW. At Q50, the corresponding far-future range is 1213.8–1521.4 MW, also reaching its maximum under SSP5-8.5. MPI-ESM1-2-HR gives a comparatively lower near-future Q40 range of 1322.5–1760.5 MW, increasing to 1753.1–2059.3 MW in the far future. Its Q50 estimates, however, show a different pattern: potential ranges from 1040.4 to 1099.2 MW in the near future and from 869.5 to 1083.5 MW in the far future. Thus, the increase in Q40-based potential is not accompanied by a consistent increase at Q50.

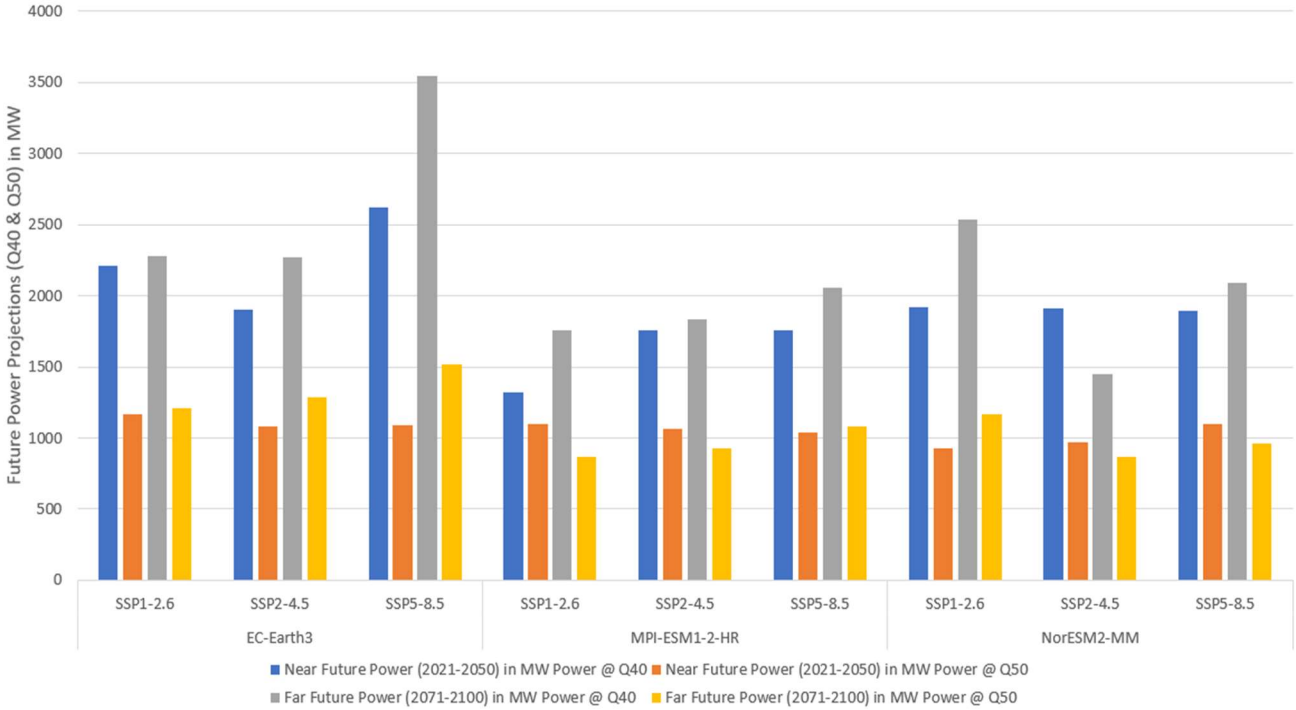


Figure 17. Future Power Projections (Q40 and Q50) under Shared Socioeconomic Pathways (SSPs).

Table 6 and Figure 17 translate the projected Q40 and Q50 discharges into theoretical power estimates using the study's head assumptions. The highest far-future Q40 estimate is 3540.8 MW for EC-Earth3 under SSP5-8.5, whereas the lowest is 1451.8 MW for NorESM2-MM under SSP2-4.5. At Q50, the far-future estimates range from 868.0 to 1521.4 MW. This spread indicates substantial model–scenario dependence. These values are theoretical estimates based on discharge and head and should not be read as actual annual electricity generation or economically developable installed capacity.

Table 6. Future Power Projections (Q40 & Q50) under SSPs.

GCM	Path	Near Future Power (2021–2050) in MW		Far Future Power (2071–2100) in MW	
		Power @ Q40	Power @ Q50	Power @ Q40	Power @ Q50
EC-Earth3	SSP1-2.6	2208.9	1165.6	2280.1	1213.8
	SSP2-4.5	1900.7	1082.7	2273.5	1282.6
	SSP5-8.5	2623.8	1093.4	3540.8	1521.4
MPI-ESM1-2-HR	SSP1-2.6	1322.5	1099.2	1753.1	869.5
	SSP2-4.5	1760.5	1066.5	1833	924.7
	SSP5-8.5	1758.4	1040.4	2059.3	1083.5
NorESM2-MM	SSP1-2.6	1917.1	927.6	2536	1165.4
	SSP2-4.5	1911.4	969.2	1451.8	868
	SSP5-8.5	1896.3	1095.7	2087.1	964.3

NorESM2-MM produces a different set of projections. Near-future Q40 power potential varies slightly, from 1896.3 to 1917.1 MW, whereas far-future values range from 1451.8 to 2536.0 MW. At Q50, potential ranges from 927.6 to 1095.7 MW in the near future and 868.0 to 1165.4 MW in the far future. SSP1-2.6 gives the highest far-future estimates under this model, at 2536.0 MW for Q40 and 1165.4 MW for Q50, while SSP2-4.5 gives the lowest values, at 1451.8 MW and 868.0 MW, respectively. This contrasts with EC-Earth3, which projects its highest far-future potential under SSP5-8.5, indicating different responses to emission pathways across climate models. Across the three GCMs and SSPs, far-future discharge ranges from 83.0 to 202.5 m^3/s at Q40 and 49.6 to 87.0 m^3/s at Q50. The associated power potential ranges from 1451.8 to 3540.8 MW at Q40 and 868.0 to 1521.4 MW at Q50 (Table 6). These represent minimum and maximum estimates among the nine model–scenario combinations, not probabilistic confidence intervals. The wide ranges highlight substantial uncertainty in future hydrological conditions and hydropower potential. Although some simulations indicate increased potential, particularly at Q40, the magnitude and direction of change depend on the climate model and scenario. Furthermore, estimated power potential does not represent actual electricity generation, as seasonal flow variability, environmental flow requirements, engineering feasibility, and operational constraints are not fully accounted for. Thus, differences among the three GCMs reflect uncertainty in climate-driven hydrological projections rather than simply contradictory results. The models represent atmospheric circulation, precipitation, temperature, and land-surface and snow-related processes differently. These differences are particularly relevant in the Dudhkoshi Basin because of its steep elevation gradient, strong monsoonal influence, snow and glacier contributions, and limited high-elevation observations [5].

The differences are more evident in the far-future period. Across all GCM–SSP combinations, Q40 ranges from 83.0 to 202.5 m^3/s, while Q50 ranges from 49.6 to 87.0 m^3/s. EC-Earth3 produces the highest Q40 under SSP5-8.5 (202.5 m^3/s), whereas NorESM2-MM gives the lowest under SSP2-4.5 (83.0 m^3/s). MPI-ESM1-2-HR shows a narrower Q40 range of 100.3–117.8 m^3/s. These differences also affect hydropower estimates, as power potential depends strongly on discharge and hydraulic head. Far-future Q40-based power ranges from 1451.8 to 3540.8 MW, representing a model–scenario range rather than a single deterministic prediction. The inter-model variations may reflect differences in projected precipitation, temperature, seasonal distribution, rainfall–snowfall partitioning, and evapotranspiration. Furthermore, downscaling and bias correction modify GCM inputs before their application in SWAT, while model parameters influence the conversion of these inputs into runoff. Therefore, no individual GCM is considered to provide the "correct" future projection; instead, the three GCMs represent a range of plausible hydrological responses. However, as precipitation, temperature, and snow-related processes were not separately quantified, their relative contributions to inter-model differences remain uncertain.

The Q40 and Q50 indicators used in this study describe flow exceedance characteristics over the selected simulation period and do not directly represent individual seasonal flow regimes. Consequently, differences in Q40 and Q50 should not be interpreted as a direct measure of changes in monsoon or pre-monsoon discharge. This distinction is particularly important for the Dudhkoshi Basin, where hydropower reliability depends not only on annual water availability but also on the timing of water availability. The projected changes indicate that future runoff conditions may differ substantially among climate models and emission pathways. However, the present analysis does not provide a dedicated monthly or seasonal decomposition of future discharge. Therefore, quantitative conclusions regarding the magnitude of monsoon enhancement or pre-monsoon reduction cannot be established from Q40 and Q50 alone. Instead, the results are interpreted as changes in flow availability at selected exceedance levels.

For run-of-river hydropower, this distinction is important because high monsoon discharge does not necessarily translate into equivalent increases in firm or dry-season energy generation. Conversely, reductions in lower-percentile flows may have a greater effect on generation reliability than increases in high-flow conditions. Previous assessments of Nepal's run-of-river hydropower system have similarly

highlighted the importance of seasonal low-flow conditions for electricity availability. Therefore, the projected Q40 and Q50 changes should be interpreted primarily as indicators of changes in hydrological availability rather than direct indicators of year-round hydropower reliability [41].

4.2. Discussions

The comparison between HEC-HMS and SWAT should be interpreted in terms of their different modelling objectives and configurations. HEC-HMS was primarily used for rainfall–runoff event simulation, whereas SWAT was configured for continuous long-term watershed simulation and subsequent climate-change and hydropower analysis. Although SWAT produced higher NSE values (0.79 calibration and 0.75 validation) than HEC-HMS (NSE 0.62 Calibration & 0.60 Validation), these results should not be interpreted as a universal ranking of model performance, as the models represent different temporal objectives and hydrological processes. SWAT was therefore used for the subsequent analyses because its continuous long-term simulation capability was required, rather than solely because of its higher NSE [21].

Here, we have made a comparison between hydropower potential sites identified during our studies and potential sites licensed by the Department of Electricity Development, Nepal (DOED). The figure indicates that the identified site does not perfectly coincide to the government-assessed locations, however, they are spatially positioned very close to each other. Currently, there are 14 licensed hydropower sites according to DOED official website (Table A1), having a power capacity of 296.275 MW. They are categorized as hydropower above 1 MW and under 1 MW. During our study we found that Dudhkoshi watershed has theoretical hydropower potential of 2992.03 MW, whereas study conducted by estimated power potential of 2741.5 M Watt at a flow exceedance probability of Q40%. These differences might be from differences in methodology, data resolution, temporal coverage, and assumptions regarding flow availability and hydropower system efficiency as well as inclusion of more micro/mini sites. The recently discovered locations were evaluated under different conditions and shed more light that can be utilized as decision tools for selecting and identifying suitable RoR hydropower projects within the Dudhkoshi Basin.

The combined analysis of EC-Earth3, MPI-ESM1-2-HR, and NorESM2-MM under various Shared Socioeconomic Pathways (SSPs) indicates a generally favorable outlook for future hydropower potential in the Dudhkoshi Basin. Under SSP1-2.6 (low emissions), all models project positive outcomes. EC-Earth3 shows stable and slightly rising flows, with Q40 power potential from 2208.9 to 2280.1 MW and Q50 above 1200 MW, supporting reliable generation. MPI-ESM1-2-HR presents lower but improving power (up to 1753.1 MW), though with possible baseflow reductions. NorESM2-MM performs strongly, projecting up to 2536 MW (Q40) in the far future, favoring low-risk, long-term development. Under SSP2-4.5 (moderate emissions), EC-Earth3 shows increased dependable flows, with Q50 power potential rising to 1282.6 MW. MPI-ESM1-2-HR and NorESM2-MM show slight declines in Q50, but Q40 values remain robust (over 1800 MW), indicating strong seasonal generation potential. In SSP5-8.5 (high emissions), EC-Earth3 projects the highest future potential, up to 3540.8 MW (Q40) and 1521.4 MW (Q50), due to greater runoff. MPI-ESM1-2-HR also improves, reaching 2059.3 MW (Q40). NorESM2-MM shows modest Q40 gains, but a Q50 decline, reflecting uncertainty in dry-season flows [2].

5. Conclusions and Future Work

This framework, comprising HEC-HMS, SWAT, and Arc GIS, provides a methodology to simulate runoff, SWAT, Arc GIS and Google Earth to identify the hydropower sites across large area basins, even in areas with limited accessibility, and to evaluate the pattern of climate change on hydropower potential power. Calibration and validation of the SWAT model for the Dudhkoshi watershed demonstrated that the model can provide reliable output for assessing hydropower potential by simulating streamflow at selected prospective sites. However, the HEC-HMS model showed only moderate performance, with a Nash–Sutcliffe Efficiency

(NSE) value of 0.62, indicating relatively lower accuracy compared to SWAT. The study region includes high elevation snow and glacier influenced areas, but limited availability of Glacier melt rate data poses a significant challenge in accurately evaluating the hydropower potential of the catchment.

A total of 47 sites, with a combined theoretical hydropower capacity of 2992.03 MW (Table A2) at 40% dependability, were, identified, representing substantial energy potential based solely on natural head and streamflow. However, the 2992.03 MW value should not be interpreted as economically or technically developable capacity. It represents the aggregate hydrological and topographic potential obtained from the screening criteria used in this study. Actual development potential would require subsequent site-specific investigations, including geological and geotechnical assessment, environmental-flow analysis, sediment and debris-flow assessment, accessibility and construction feasibility, transmission-grid availability, economic analysis, land requirements, and environmental and social impact assessment. The present analysis is therefore best regarded as a preliminary basin-scale screening exercise to identify locations that warrant further investigation, rather than as a project-development inventory [3].

Together, under climate change, the SSP1-2.6 climate pathway for each of the GCMs indicates that green climate interventions can ensure or enhance hydropower potential for the Dudhkoshi Basin. While there are model-specific variations in seasonal discharge distribution, the overall trend is indicative of the viability and robustness of hydropower projects under a low-emission future. These findings strongly support using multi-model and multi-scenario information in future hydropower planning. However, the projected changes represent hydrological and topographic potential rather than guaranteed electricity generation or economically developable capacity. Future assessments should incorporate seasonal firm-flow analysis, environmental-flow requirements, sediment and geological conditions, infrastructure accessibility, transmission constraints, project economics, and environmental and social considerations [23].

Appendix A

Table A1. Licensed Hydropower List From DOED.

SN	Project	River	Intake/Power House Co-Ordinates				Capacity (MW)
			Intake/Power ID	Latitude	Longitude	Elevation (m)	
1	Salleri Chialsa	Solu Khola	2-L	27.48694	86.58333	2430.1	0.6
			2-F	27.48028	86.56944	2036.9	
2	Junbeshi	Junbeshi	7-L	27.58556	86.57472	3291.7	5.2
			7-F	27.55417	86.54444	3199.4	
3	Rawa Khola HPP	Rawa Khola	16-L	27.31417	86.75861	779.6	6.5
			16-F	27.2975	86.7375	816.8	
4	Lower Solu Hydropower Project	Solu Khola	17-L	27.44472	86.62611	2423.4	82
			17-F	27.41361	86.57528	2782.2	
5	Mid Rawa Khola HEP	Rawa Khola, Sung Khola	122-L	27.35111	86.84806	1222.9	2.5
			122-F	27.34	86.81806	1264.1	
6	Dudhkoshi-2 (Jaleswar) HPP	Dudh Koshi	123-L	27.44167	86.72667	1180.9	70
			123-F	27.39778	86.66667	1204.3	
7	Lower Mid Rawa Khola HEP	Rawa	125-L	27.35	86.81667	1181.1	4
			125-F	27.33417	86.78028	952.8	
8	Middle Hongu Khola B HEP	Hongu Khola	152-L	27.51417	86.85944	1535.2	22.9
			152-F	27.48583	86.81833	1788.9	
9	Madhya Hongu Khola -A HPP	Hongu Khola	162-L	27.53556	86.89833	2047.6	22
			162-F	27.51417	86.85639	1485.3	
10	Luja Khola HEP	Luja Khola	176-L	27.69611	86.71667	2637.9	24.8
			176-F	27.66222	86.67778	3190.9	

11	Budum HEP	budum	183-L	27.50361	86.86389	2180.4	14.5
			183-F	27.46944	86.83194	2805.9	
12	Upper Junbesi Khola HEP	Junbeshi	215-L	27.61111	86.55667	3248.1	5.875
			215-F	27.59083	86.53333	3550.3	
13	Rawa Khola HEP	Rawa	235-L	27.3375	86.78333	890.1	5.4
			235-F	27.315	86.75833	732.5	
14	Hongu Khola I HEP	Hongu Khola	238-L	27.49417	86.81833	1290	30
			238-F	27.475	86.76361	1083.3	
Source: https://doed.gov.np/license/54 (accessed on 30 October 2024)							296.275

Table A2. Identified Hydropotential Sites in Dudhkoshi River Basin.

SN	Intake ID	Longitude	Latitude	Elevation (m)	Power House ID	Longitude	Latitude	Elevation (m)	HEAD Diff (m)	Catch. Area (km^2)	HEAD (m)	Q40 Discharge	Capacity (MW)
1	O101	86.797	27.479	1732.8	P101	86.7645	27.4727	1212.5	520.3	560	520.35	31.37	160.13
2	O102	86.7583	27.4521	1829.8	P102	86.729	27.4531	861.2	968.6	2000	968.63	98.64	937.33
3	O103	86.8707	27.3755	1483.4	P103	86.862	27.362	1322.1	161.3	41	161.26	2.98	4.72
4	O104	86.8567	27.3601	1282.7	P104	86.8473	27.3533	1186.4	96.3	13	96.26	1.06	1
5	O106	86.8309	27.3452	1070.9	P106	86.7819	27.3362	881	189.9	88	189.93	5.93	11.05
6	O107	86.792	27.3698	1138.3	P107	86.7788	27.3453	908.8	229.5	46	229.53	3.31	7.45
7	O109	86.8809	27.3031	1474.8	P109	86.8415	27.3024	1119	355.8	69	355.82	4.77	16.63
8	O110	86.8326	27.3034	1180.1	P110	86.7775	27.3196	821.6	358.5	120	358.49	7.84	27.58
9	O112	86.7513	27.3147	707.4	P112	86.7389	27.3069	645.136	62.264	340	62.26	20.02	12.23
10	O123	86.7405	27.3086	657.4	P123	86.7252	27.2979	610.1	47.3	350	47.3	20.55	9.53
11	O125	86.7012	27.289	546.8	P125	86.6824	27.2734	476	70.8	390	70.75	22.65	15.72
12	O126	86.6797	27.3562	569.3	P126	86.6828	27.3193	508.993	60.307	3300	60.34	154.81	91.63
13	O16	86.7194	27.7872	2827.6	P16	86.7214	27.7705	2736.1	91.5	1100	91.55	57.6	51.73
14	O32	86.713	27.7509	2646.2	P32	86.7108	27.7403	2607.7	38.5	1200	43.3	62.29	26.46
15	O33	86.7107	27.7401	2594.7	P33	86.712	27.7192	2505.7	89	1200	88.94	62.29	54.34
16	O34	86.7116	27.7116	2496.4	P34	86.7108	27.6898	2258.9	237.5	1300	237.57	66.94	156.01
17	O35	86.715	27.6778	2081.4	P35	86.7049	27.6617	1903.4	178	1300	177.99	66.94	116.88
18	O38	86.6942	27.6145	1567.5	P38	86.68	27.5977	1493.9	73.6	1500	73.58	76.14	54.96
19	O39	86.6491	27.5966	1847.3	P39	86.6732	27.5941	1594.3	253	22	252.99	1.7	4.23
20	O40	86.6782	27.5926	1483.4	P40	86.6756	27.5713	1401.7	81.7	1500	81.74	76.14	61.06
21	O41	86.6797	27.5657	1331.3	P41	86.6985	27.5599	1259.1	72.2	1600	72.19	80.69	57.14
22	O42	86.7033	27.5549	1237.2	P42	86.7109	27.5333	1158	79.2	1600	79.24	80.69	62.73
23	O43	86.6496	27.491	1543.6	P43	86.6886	27.4913	1235.2	308.4	27	308.47	2.05	6.2
24	O44	86.6932	27.4908	996	P44	86.7168	27.4782	922.8	73.2	1700	73.2	85.22	61.19
25	O52	86.8	27.6174	2917.8	P52	86.791	27.6113	2505	412.8	210	412.77	12.98	52.54
26	O53	86.7893	27.6082	2475.2	P53	86.7854	27.5929	2109	366.2	220	366.2	13.53	48.61
27	O55	86.782	27.5779	1937	P55	86.7682	27.5592	1678.1	258.9	250	258.93	15.18	38.56
28	O57	86.7588	27.5314	1294.8	P57	86.7304	27.4905	964.2	330.6	280	330.56	16.81	54.51
29	O60	86.5973	27.5868	2573.4	P60	86.5921	27.5695	2485.7	87.7	95	87.76	6.35	5.47
30	O61	86.5903	27.5652	2442.2	P61	86.5798	27.5501	2368.7	73.5	110	73.54	7.25	5.23

31	O62	86.5828	27.5451	2382.8	P62	86.5784	27.5252	2194.8	188	210	187.96	12.98	23.93
32	O63	86.5414	27.6053	2942.3	P63	86.5478	27.5799	2644	298.3	53	298.32	3.76	11
33	O64	86.5523	27.5683	2562.1	P64	86.5747	27.5514	2379.2	182.9	83	182.93	5.63	10.1
34	O66	86.5728	27.482	2113.4	P66	86.5676	27.4606	1919.5	193.9	290	193.87	17.35	33
35	O67	86.5764	27.4404	2015.2	P67	86.6032	27.4354	1662	353.2	420	353.25	24.21	83.91
36	O68	86.496	27.4592	2224.6	P68	86.5135	27.4472	2111.8	112.8	50	112.76	3.57	3.94
37	O70	86.6129	27.4264	1575.2	P70	86.6279	27.4011	1077.6	497.6	440	497.53	25.25	123.23
38	O71	86.6334	27.391	976.2	P71	86.6494	27.3786	824	152.2	490	152.16	27.82	41.52
39	O73	86.723	27.4712	885.9	P73	86.7255	27.4535	837.9	48	2000	48.04	98.64	46.48
40	O75	86.7145	27.4414	790.8	P75	86.6969	27.4309	746.205	44.595	2600	44.64	124.91	54.7
41	O76	86.6981	27.4317	758.6	P76	86.6852	27.4112	691.6	67	2600	67.03	124.91	82.14
42	O77	86.6845	27.4108	681.5	P77	86.6812	27.392	637	44.5	2700	44.5	129.23	56.42
43	O95	86.9086	27.5963	2361.5	P95	86.8963	27.5716	1978.4	383.1	290	383.03	17.35	65.19
44	O96	86.8967	27.5669	1925.1	P96	86.893	27.548	1738.4	186.7	330	186.77	19.49	35.71
45	O97	86.892	27.5351	1638.4	P97	86.8779	27.523	1491.6	146.8	370	146.86	21.6	31.12
46	O98	86.871	27.5186	1467.5	P98	86.8457	27.5125	1342.1	125.4	420	125.37	24.21	29.78
47	O99	86.8405	27.5093	1324.9	P99	86.8215	27.4994	1238	86.9	470	86.92	26.79	22.84
							Capacity (MW)						2992.03

Statement of the Use of Generative AI and AI-Assisted Technologies in the Writing Process

During the preparation of this manuscript, the authors used ChatGPT to aid proofreading and grammatical corrections. After using this tool/service, the authors reviewed and edited the content as needed and take full responsibility for the content of the published article.

Acknowledgments

The authors are grateful to all faculty members of the Institute of Engineering, Purwanchal Engineering Campus, and to the Department of Hydrology and Meteorology (DHM), Government of Nepal, for providing the hydrometeorology data used in this study.

Author Contributions

Conceptualization, S.K. (Sambridhi Karki) and B.P.S.; Methodology, S.K. (Sambridhi Karki) and A.D.; Software, S.K. (Sambridhi Karki).; Validation, S.K. (Sambridhi Karki), A.D. and B.P.S.; Formal Analysis, S.K. (Saroj Karki); Investigation, S.K. (Sambridhi Karki) and B.P.S.; Resources, S.K. (Saroj Karki).; Data Curation, S.K. (Saroj Karki).; Writing—Original Draft Preparation, S.K. (Sambridhi Karki) and B.P.S.; Writing—Review & Editing, S.K. (Sambridhi Karki), B.P.S. and S.K. (Saroj Karki); Visualization, S.K. (Sambridhi Karki) ; Supervision, A.D.

Ethics Statement

Not Applicable.

Informed Consent Statement

Not applicable.

Data Availability Statement

The datasets used and analyzed in this study, including meteorological data, observed river discharge data, spatial datasets (DEM, land use/land cover, and soil data), and hydrological model outputs, are available from the corresponding author upon reasonable request. Climate projection data used in this study are available from the respective CMIP6 data providers

Funding

This research received no external funding.

Declaration of Competing Interest

The authors declare that they have no known competing financial interests or personal relationships that could have appeared to influence the work reported in this paper.

References

1. Jha R. Total Run-of-River type Hydropower Potential of Nepal. *Hydro Nepal J. Water Energy Environ.* **1970**, *7*, 8–13. DOI:10.3126/hn.v7i0.4226
2. Prajapati RN, Ibrahim N, Thapa BR. Climate change impact on water availability in the Himalaya: Insights from Sunkoshi River basin, Nepal. *HydroResearch* **2023**, *6*, 279–292. DOI:10.1016/j.hydres.2023.10.002
3. Lamichhane S, Devkota N, Subedi TR, Thapa AB. Impact of land use and land cover change in river flow and hydro-energy generation: The case of Bagmati basin in central Nepal. *Energy Nexus* **2024**, *14*, 100305. DOI:10.1016/j.nexus.2024.100305

4. Subedi SR, Lamichhane M, Dhungana S, Chalise B, Bhattarai S, Chaulagain U, et al. Assessing the impact of climate change on streamflow in the Tamor River Basin, Nepal: An analysis using SWAT and CMIP6 scenarios. *Discover. Civ. Eng.* **2024**, *1*, 135. DOI:10.1007/s44290-024-00143-2
5. Wester P, Mishra A, Mukherji A, Shrestha AB. *The Hindu Kush Himalaya Assessment: Mountains, Climate Change, Sustainability and People*; Springer: Cham, Switzerland, 2019. DOI:10.1007/978-3-319-92288-1
6. Jha AN, Ansari A, Khatakho R, Shrestha E, Suwal N, Ankon SB, et al. Climate change impacts on tributary-scale water-balance partitioning and hydrological resilience in the Koshi River Basin, Himalaya. *H2Open J.* **2026**, *9*, 100092. DOI:10.1016/j.htopen.2026.100092
7. Adhikari D, Upadhaya M, Khadka N, Shah DN, Thapa LB, Yadav RKP, et al. Hydroclimatic Changes in the Marsyangdi River Basin, Central Himalaya Under CMIP6 Scenarios: Implications for the Water–Energy–Food–Ecosystem Nexus. *Meteorol. Appl.* **2026**, *33*, e70240. DOI:10.1002/met.70240
8. Bista S, Singh U, Kayastha N, Ghimire BNS, Talchabhadel R. Effects of Source Digital Elevation Models in Assessment of Gross Runoff-River Hydropower Potential: A Case Study of West Rapti Basin, Nepal. *J. Eng. Iss. Solut.* **2021**, *1*, 106–128. DOI:10.3126/joeis.v1i1.36822
9. Thapa B, Danegulu A, Suwal N, Upadhyay S, Manandhar B, Prajapati R. Rainfall-Runoff Modelling of the West Rapti Basin, Nepal. *Tech. J.* **2020**, *2*, 99–107. DOI:10.3126/tj.v2i1.32846
10. Pokharel N, Basnet K, Sherchan B, Thapaliya D. Assessment of Hydropower Potential using SWAT modeling and Spatial Technology in the Seti Gandaki River, Kaski, Nepal. *IEEE-SEM* **2020**, *8*, 87–102. Available online: https://docslib.org/doc/76739/assessment-of-hydropower-potential-using-swat-modeling-and-spatial-technology-in-the-seti-gandaki-river-kaski-nepal (accessed on 29 October 2026).
11. Bhattarai R, Mishra BK, Bhattarai D, Khatiwada D, Kumar P, Meraj G. Assessing Hydropower Potential in Nepal's Sunkoshi River Basin: An Integrated GIS and SWAT Hydrological Modeling Approach. *Scientifica* **2024**, *2024*, 1007081. DOI:10.1155/2024/1007081
12. Ahmadzadeh Kaleybar F, Emarat-Pardaz J. Estimating of Flood Hydrograph Using HEC-HMS Model. In Proceedings of the International Conference on Natural Disasters and Human Life Safety, Baku, Azerbaijan, 5–6 December 2017.
13. Shrestha M, Acharya SC, Shrestha PK. Bias correction of climate models for hydrological modelling—Are simple methods still useful? *Meteorol. Appl.* **2017**, *24*, 531–539. DOI:10.1002/met.1655
14. Shrestha S, Khatiwada M, Babel MS, Parajuli K. Impact of Climate Change on River Flow and Hydropower Production in Kulekhani Hydropower Project of Nepal. *Environ. Process.* **2014**, *1*, 231–250. DOI:10.1007/s40710-014-0020-z
15. Maharjan S, Li W, Fazli S, Ansari A, Tiwari S, Thakurathi R, et al. Unfolding cascading impacts of changing South Asia monsoon on a Hindu Kush Himalayas basin. *J. Hydrol. Reg. Stud.* **2025**, *57*, 102155. DOI:10.1016/j.ejrh.2024.102155
16. Adhikary S, Aryal M. Spatial heterogeneity in basin hydrology and hydropower potential: Implications for climate resilience and economic development in Nepal. *River* **2026**, *5*, 265–281. DOI:10.1002/rvr2.70055
17. Sharma N. *River System Analysis and Management*; Springer: Singapore, 2017. DOI:10.1007/978-981-10-1472-7
18. Budhathoki BR, Adhikari TR, Shrestha S, Awasthi RP, Dawadi B, Gao H, et al. Application of hydrological models to streamflow estimation at ungauged transboundary Himalayan River basin, Nepal. *Hydrol. Res.* **2024**, *55*, 859–872. DOI:10.2166/nh.2024.026
19. Malhotra A. Applicability of TRMM Precipitation for Hydrological Modeling Using HEC-HMS in Karnali River Basin in Nepal. *J. Adv. Coll. Eng. Manag.* **2023**, *8*, 45–58. DOI:10.3126/jacem.v8i1.55910
20. Jha AN, Bhattarai U, Lamichhane M, Mehan S, Ghimire S, Bhattarai PK. Assessing hydropower production potential with multisite hydrological modeling in the Koshi river Basin, Nepal. *Energy Convers. Manag. X* **2025**, *28*, 101283. DOI:10.1016/j.ecmx.2025.101283
21. Joshi TP, Mishra BK. Assessment of Run-of-River Hydropower Potential Using SWAT Modeling and GIS in the Marsyangdi River Basin, Nepal. *J. Hydrol. Meteorol.* **2024**, *12*, 11–22. DOI:10.3126/jhm.v12i1.72651
22. Adhikari P, Mishra BK, Baral S. Sediment yield assessment in the Budhi Gandaki Basin Nepal using the SWAT model. *Discover. Geosci.* **2026**, *4*, 147. DOI:10.1007/s44288-026-00518-1
23. Marasini U, Pokhrel M. Comparative analysis of rainfall-runoff simulation using a long short-term memory (LSTM) deep learning model and a conceptual hydrological model, HEC-HMS: A case study of the mountainous river basin of Nepal. *Discover. Civ. Eng.* **2024**, *1*, 78. DOI:10.1007/s44290-024-00084-w
24. Bhatta B, Shrestha S, Shrestha PK, Talchabhadel R. Evaluation and application of a SWAT model to assess the climate change impact on the hydrology of the Himalayan River Basin. *Catena* **2019**, *181*, 104082. DOI:10.1016/j.catena.2019.104082

25. Poudel S, Ramtel P. Assessing climate change impacts on design of small hydropower projects in Nepal using a process-based hydrological model with machine learning post-processor. *J. Water Clim. Change* **2026**, *17*, 1383–1399. DOI:10.2166/wcc.2026.437
26. Nakhaei P, Kisi O, Nakhaei M, Fathollahi-Fard AM, Gheibi M. Assessment of climate change on river streamflow under different representative concentration pathways. *J. Environ. Manag.* **2024**, *366*, 121754. DOI:10.1016/j.jenvman.2024.121754
27. Ghazikhani A, Babaeian I, Gheibi M, Hajiaghaei-Keshteli M, Fathollahi-Fard AM. A Smart Post-Processing System for Forecasting the Climate Precipitation Based on Machine Learning Computations. *Sustainability* **2022**, *14*, 6624. DOI:10.3390/su14116624
28. Kumar N, Dubey AK, Goswami UP, Singh SK. Modelling of hydrological and environmental flow dynamics over a central Himalayan river basin through satellite altimetry and recent climate projections. *Int. J. Climatol.* **2022**, *42*, 8446–8471. DOI:10.1002/joc.7734
29. Baral K, Pandey VP, Pradhan AMS. Impact on Hydrological Alteration due to Climate Change in Seti Watershed. *J. UTEC Eng. Manag.* **2024**, *2*, 25–35. DOI:10.36344/utecem.2024.v02i01.003
30. Pradhananga S, Nepal S, Kamal SK, Hafeez M. Climate change will exacerbate seasonal flow variability in the Karnali River basin: Implications for water, energy, and agriculture sectors. *Hydrol. Res.* **2025**, *56*, 471–491. DOI:10.2166/nh.2025.193
31. Kisi O, Choubin B, Deo RC, Yaseen ZM. Incorporating synoptic-scale climate signals for streamflow modelling over the Mediterranean region using machine learning models. *Hydrol. Sci. J.* **2019**, *64*, 1240–1252. DOI:10.1080/02626667.2019.1632460
32. Chaulagain D, Ray RL, Yakub AO, Same NG, Jong JP, Roh W, et al. Impacts of climate change on hydrological patterns and implications for hydroelectric power generation in Khimti River Basin, Nepal. *Discover. Appl. Sci.* **2025**, *7*, 688. DOI:10.1007/s42452-025-07304-7
33. O'Neill BC, Tebaldi C, van Vuuren DP, Eyring V, Friedlingstein P, Hurtt G, et al. The Scenario Model Intercomparison Project (Scenario MIP) for CMIP6. *Geosci. Model Dev.* **2016**, *9*, 3461–3482. DOI:10.5194/gmd-9-3461-2016
34. U.S. Army Corps of Engineers. *HEC-HMS Technical Reference Manual*; Hydrologic Engineering Center: Davis, CA, USA, 2026.
35. Arnold JG, Srinivasan R, Muttiah RS, Williams JR. Large Area Hydrologic Modeling and Assessment Part I: Model Development. *J. Am. Water Resource. Assoc.* **1998**, *34*, 73–89. DOI:10.1111/j.1752-1688.1998.tb05961.x
36. Moriasi DN, Arnold JG, Van Liew MW, Bingner RL, Harmel RD, Veith TL. Model Evaluation Guidelines for Systematic Quantification of Accuracy in Watershed Simulations. *Trans. ASABE* **2007**, *50*, 885–900. DOI:10.13031/2013.23153
37. Kayastha N, Singh U, Dulal KP. A GIS Approach for Rapid Identification of Run-of-River (RoR) Hydropower Potential Site in Watershed: A case study of Bhote Koshi Watershed, Nepal. *Hydro Nepal J. Water Energy Environ.* **2018**, *23*, 48–55. DOI:10.3126/hn.v23i0.20825
38. Bieger K, Arnold JG, Rathjens H, White MJ, Bosch DD, Allen PM, et al. Introduction to SWAT+, A Completely Restructured Version of the Soil and Water Assessment Tool. *J. Am. Water Resource. Assoc.* **2016**, *53*, 115–130. DOI:10.1111/1752-1688.12482
39. Poudel A, Bhattarai U, Suwal N, Kuriqi A. Water, Watt, and Warming: Hydropower Futures in the Eastern Nepal Himalayas under Climate Change. *J. Water Clim. Change* **2026**, *17*, 1853–1882. DOI:10.2166/wcc.2026.359
40. Nash JE, Sutcliffe JV. River flow forecasting through conceptual models' part I—A discussion of principles. *J. Hydro.* **1970**, *10*, 282–290. DOI:10.1016/0022-1694(70)90255-6
41. Arnold JG, Moriasi DN, Gassman PW, Abbaspour KC, White MJ, Srinivasan R, et al. SWAT: Model Use, Calibration, and Validation. *Trans. ASABE* **2012**, *55*, 1491–1508. DOI:10.13031/2013.42256